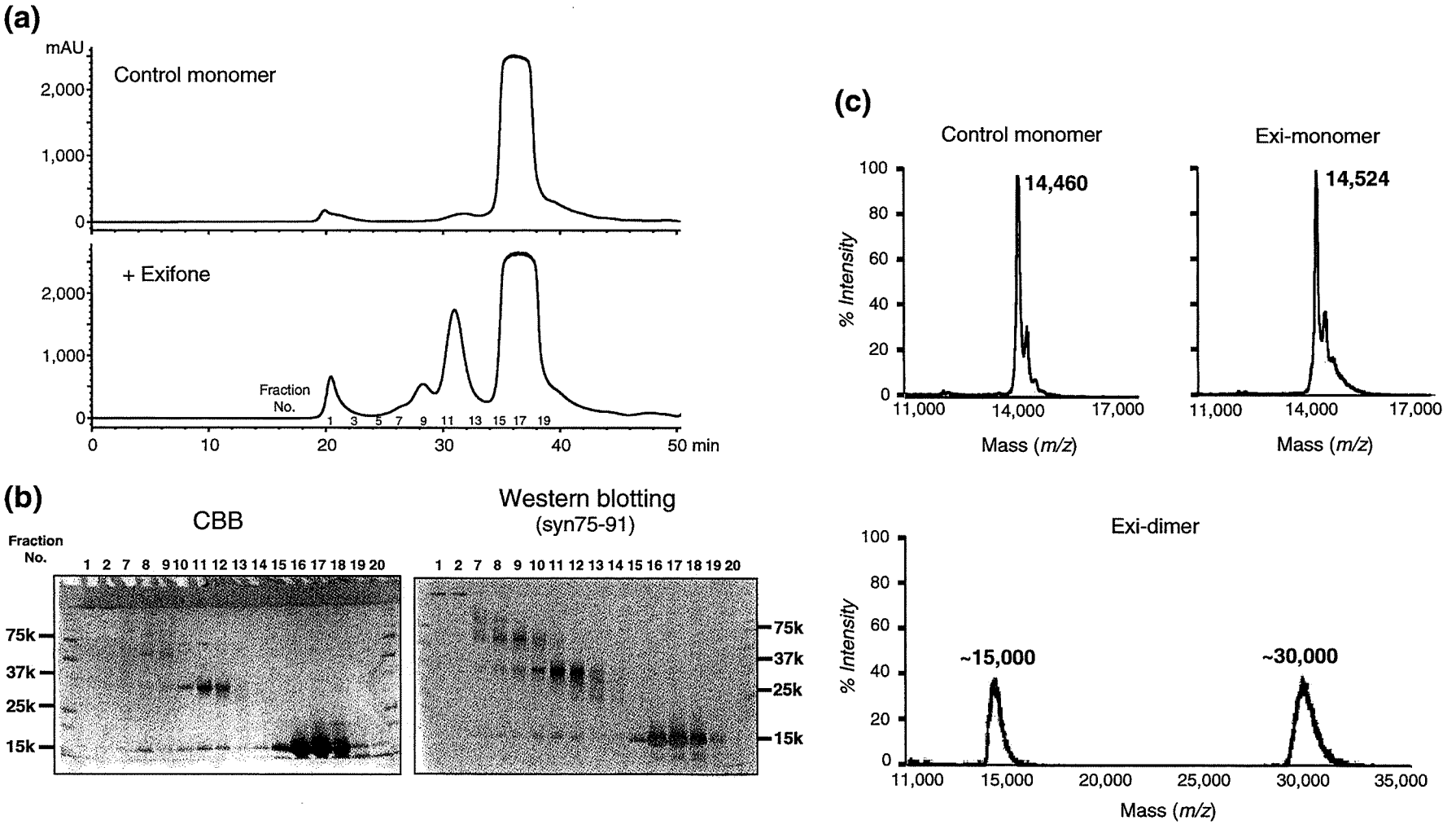

Fig. 2. Isolation and characterization of exifone-bound α-synucleins. (a) Separation of exifone-treated α-synuclein monomer and dimer by gel-filtration chromatography (detection: absorbance at 214 nm). (b) SDS-PAGE of fractions separated by gel-filtration chromatography (Coomassie brilliant blue staining and Western blotting). Pooled fractions 11–12 and 16–18 were used as Exi-dimer and Exi-monomer, respectively. (c) Partial MALDI-TOF MS spectra of α-synuclein monomer (control), Exi-monomer, and Exi-dimer.

contains one exifone molecule per α-synuclein chain (Supplementary Fig. S1).

For the identification of the modification (corresponding to a molecular mass of 64 Da) found in the Exi-monomer, α-synuclein was incubated with various concentrations of exifone (0, 0.2, 0.5, 1, and 2 mM) and the resulting samples were analyzed by MS (Supplementary Fig. S2). The molecular mass of α-synuclein increased in an exifone concentration-dependent manner and reached 14,528 Da (Supplementary Fig. S2a and b). A similar increase in molecular mass was reported in the presence of H_2O_2, which oxidized methionine residues to methionine sulfoxide.[14] Methionine oxidation is known to increase mass by 16 Da. α-Synuclein has four methionine residues, Met1, Met5, Met116, and Met127, and thus the oxidation of all the methionine residues would result in an increase in mass of 64 Da (Supplementary Fig. S3c). Indeed, α-synuclein incubated with various concentrations of H_2O_2 showed a concentration-dependent increase in molecular mass of up to 14,533 Da (Supplementary Fig. S3a and b), similar to that seen in the case of exifone. These results strongly suggest that all the methionine residues of Exi-monomer were oxidized to methionine sulfoxide.

Peptide mapping of inhibitor-induced α-synuclein dimer and monomer

In order to confirm the oxidation of methionine, control α-synuclein, Exi-monomer, Exi-dimer, and H_2O_2-treated α-synuclein monomer were digested with trypsin, and the resulting peptide mixtures were analyzed by reverse-phase HPLC (Fig. 3a). The elution patterns of peptides derived from Exi-monomer and Exi-dimer exhibited different profiles compared with that of control α-synuclein. Peaks 5 and 10 in the map of control α-synuclein were absent in the maps of Exi-monomer and Exi-dimer. Instead, peaks 11–18 newly appeared in the maps of Exi-monomer and Exi-dimer. The patterns of Exi-monomer and Exi-dimer were similar to those of α-synuclein oxidized with H_2O_2. All the peaks were analyzed by MS and the results are summarized in Fig. 3b. Peaks 5 and 10 were identified as Met1–Lys6 (containing two methionines, Met1 and Met5) and Asn103–Ala140 (containing Met116 and Met127), respectively. In the case of Exi-monomer or Exi-dimer, peaks 11, 15, and 19 were identified as Met1–Lys6 including two oxidized methionines. Peaks 12, 16, and 20 were identified as Asn103–Ala140 including oxidized Met116 and Met127. Peaks 13, 14, 16, and 17 were derived from Asn103–Ala140 oxidized at either Met116 or Met127. Similar results were obtained for dopamine-bound dimer and monomer (data not shown). These results clearly indicate that the inhibitors exifone and dopamine have the ability to oxidize methionine residues on α-synuclein. It is established that α-synuclein assembly was inhibited by exifone at low micromolar range (IC_{50}=2.5 μM),[3] and methionine sulfoxide could not be detected at a low concentration of exifone (data not shown). These findings suggest that the stabilization of intermediate oligomers by small molecules is responsible for the inhibition of filament formation, and oxidation of methionine does not seem to play a major role in inhibition.

No covalent inhibitor–peptide adducts or cross-linked peptides were detected in the peptide mapping experiments, indicating that the inhibitors bind noncovalently to α-synuclein and that α-synuclein dimer is formed in a noncovalent fashion. These observations are consistent with the results of MALDI MS analysis of Exi-monomer, which showed no inhibitor adducts (Fig. 2c). Our extensive liquid chromatography–electrospray ionization MS analysis also did not show the covalent inhibitor adducts or α-synuclein dimer (data not shown). Further, more detailed biochemical studies to investigate the modes of inhibitor binding and dimerization are currently in progress.

Characterization of exifone-binding regions in α-synuclein

Exifone is an antioxidant and thus can be detected by redox-cycling staining, which is a well-established method for detecting quinoproteins.[15] As expected, Exi-dimer and Exi-monomer were stained as purple bands by redox-cycling staining due to nitroblue tetrazolium (NBT) reduction to formazan (Fig. 4a), while untreated control α-synuclein showed no staining. This result shows that redox-cycling staining is useful for examining the exifone-binding regions in α-synuclein. In order to determine the binding region of exifone and the regions involved in the dimerization, Exi-dimer was digested with endoproteinase Asp-N and the resulting peptides were detected with silver or redox-cycling staining. Asp-N digestion of Exi-dimer gave two major fragments, corresponding to molecular masses of 20 kDa (no. 1) and 16 kDa (no. 2), on SDS-PAGE after silver staining (Fig. 4b). These two bands were positive for redox-cycling staining. Since α-synuclein monomer migrates at 15 kDa, these fragments represent dimeric peptides stabilized by exifone. α-Synuclein has six aspartic acid residues (Asp2, Asp98, Asp115, Asp119, Asp121, and Asp135). Immunoblot analysis with a panel of site-specific anti-α-synuclein antibodies (Fig. 5) suggested that the 20-kDa fragment contains the dimerized N-terminal fragment Met1–Met97 of α-synuclein (cleaved at the N-terminus of Asp98). The 16-kDa fragment was also labeled with antibodies to the N-terminal and central portions of α-synuclein (residues 1–50). It has been reported that Asp-N cleaves peptide bonds N-terminal to glutamate as well as aspartate residues.[16,17] Glu57 and/or Glu61 are found in the middle of α-synuclein and are candidate Asp-N cleavage sites to produce the 16-kDa fragment. The reactivity of anti-α-synuclein antibodies and the relaxed specificity of Asp-N indicate that the 16-kDa fragment corresponds to a dimer composed of Met1–Ala56/Lys60. These results suggest that the N-terminal region (1–60) of α-synuclein is involved in

the dimerization and exifone binding. This is in contrast with a previous report by Norris *et al.*, in which they suggested that dopamine inhibited the aggregation of α-synuclein by binding to the C-terminal residues 125–129 (i.e., YEMPS) and stabilizing the soluble oligomers.[6] The discrepancy might be due to the fact that they analyzed the dopamine-binding sites by using deletion mutants lacking the C-terminal regions and did not use full-length α-synucleins.

High-resolution NMR spectra of inhibitor-bound α-synuclein monomer and dimer

In order to characterize the behavior of α-synuclein monomer and dimer formed in the presence of polyphenolic compounds, we conducted a structural analysis of inhibitor-bound α-synuclein monomer and dimer using ultra-high-field NMR spectroscopy. NMR signals of backbone amides constitute excellent probes to provide maps of the interacting sites and to examine the effects of modifications.[13] Fig. 6a and b shows the ^{1}H–^{15}N heteronuclear single quantum coherence (HSQC) spectra of uniformly ^{15}N-labeled Exi-monomer and Exi-dimer, as well as control monomer, recorded at a proton observation frequency of 920 MHz. The amide resonances of Exi-monomer and Exi-dimer were assigned by comparing the NMR spectral data with those of control α-synuclein monomer. Little chemical shift difference was detected between Exi-monomer and control monomer for most observed peaks, except for the signals corresponding

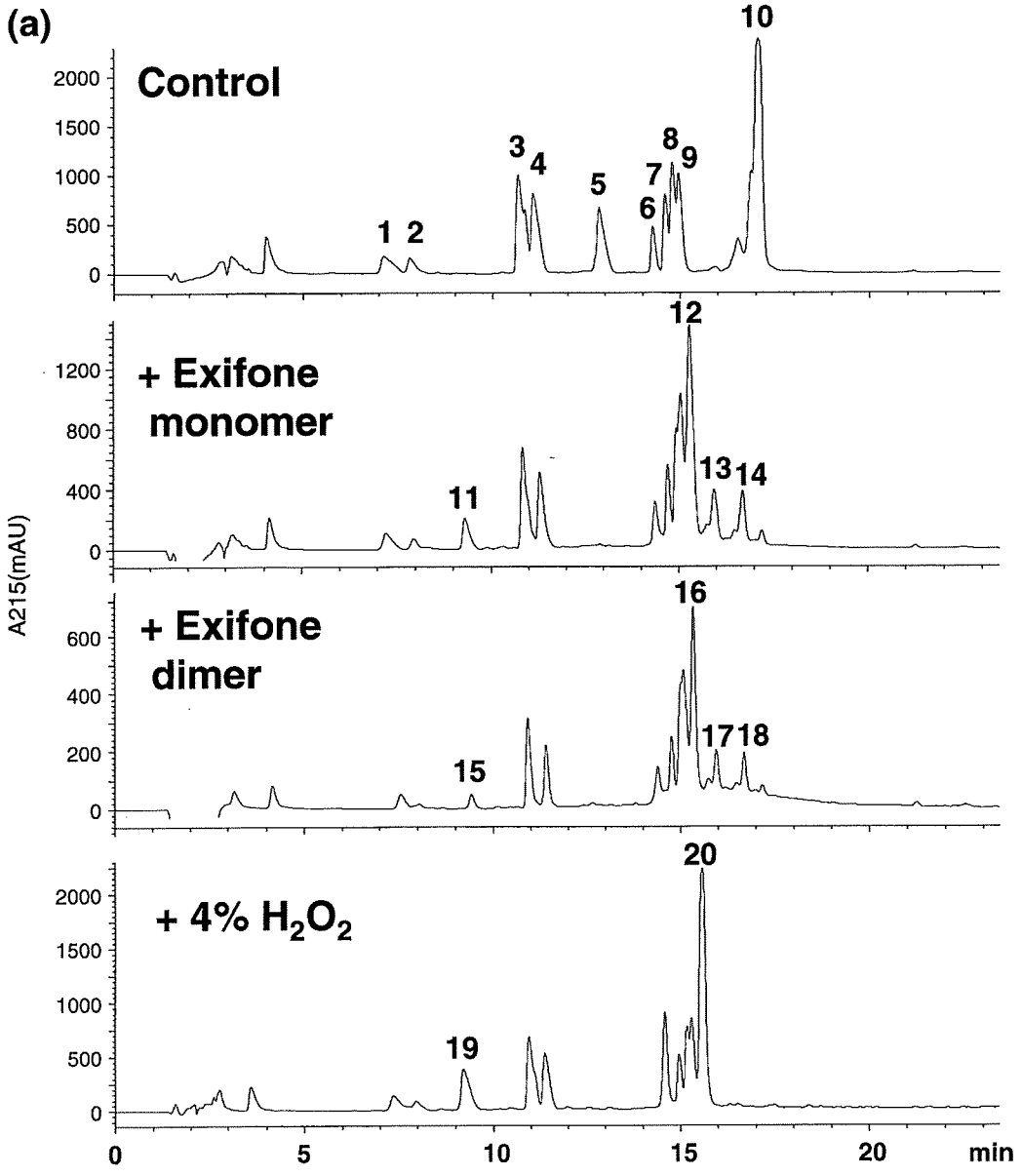

Fig. 3. Tryptic peptide mapping and MS analysis of α-synucleins. (a) Reverse-phase HPLC patterns of monomeric α-synuclein (control), Exi-monomer, Exi-dimer, and H_2O_2-treated α-synuclein monomer. (b) Observed masses and peak assignments of the peptides separated on a reverse-phase column. Oxidation of methionine residues was observed in Exi-monomer and Exi-dimer, as well as H_2O_2-treated α-synuclein monomer.

(b)

Peak No.	$(M+H)^+$ Observed	$(M+H)^+$ Calculated	Assignment
1	830.6 873.5 1072.6	830.4 873.4 1072.5	QGVAEAAGK (24-32) EGVVAAAEK (13-21) AKEGVVAAAEK (11-21)
2	1180.7 1295.8 1524.8	1180.6 1295.6 1524.8	TKEGVLYVGSK (33-43) EGVVHGVATVAEK (46-58) TKEGVVHGVATVAEK (44-58)
3	951.5	951.5	EGVLYVGSK (35-43)
4	1295.7	1295.6	EGVVHGVATVAEK (46-58)
5	770.5	770.3	MDVFMK (1-6)
6	1606.6	1606.8	TVEGAGSIAAATGFVKK (81-97)
7	2157.2	2157.1	TKEQVTNVGGAVVTGVTAVAQK (58-80)
8	1478.5	1478.7	TVEGAGSIAAATGFVK (81-96)
9	1928.0	1928.0	EQVTNVGGAVVTGVTAVAQK (61-80)
10	4295.0	4286.7	NEEGAPQEGILEDMPVDPDNAYEMPSEEGYQDYEPEA (103-140)
11	803.0	802.3.0	M*DVFM*K (1-6) (M*:methionine sulfoxide)
12	4322.0	4318.7	NEEGAPQEGILEDM*PVDPDNAYEM*PSEEGYQDYEPEA (103-140)
13	4311.0	4302.7	NEEGAPQEGILEDM#PVDPDNAYEM#PSEEGYQDYEPEA (103-140) (One of two methionine residues (M#) was oxidized)
14	4312.0	4302.7	NEEGAPQEGILEDM#PVDPDNAYEM#PSEEGYQDYEPEA (103-140)
15	802.0	802.3	M*DVFM*K (1-6)
16	4322.0	4318.7	NEEGAPQEGILEDM*PVDPDNAYEM*PSEEGYQDYEPEA (103-140)
17	4311.0	4302.7	NEEGAPQEGILEDM#PVDPDNAYEM#PSEEGYQDYEPEA (103-140)
18	4312.0	4302.7	NEEGAPQEGILEDM#PVDPDNAYEM#PSEEGYQDYEPEA (103-140)
19	803.0	802.3	M*DVFM*K (1-6)
20	4322.0	4318.7	NEEGAPQEGILEDM*PVDPDNAYEM*PSEEGYQDYEPEA (103-140)

Fig. 3 *(legend on previous page)*

to Met5, Met116, Met127, and their neighboring residues (Fig 6a). The observed chemical shift differences are mostly attributable to the oxidation of methionine residues. The differences in peak intensities between Exi-monomer and control monomer were also generally small (Fig. 6c). These results indicate that the dynamical features of both synuclein monomers are almost the same, and methionine oxidation itself does not greatly influence the structural characteristics of α-synuclein.

It is noteworthy that significant reductions in signal intensity [I(Exi-dimer)/I(control monomer)< 0.8] were observed for the peaks originating from the N-terminal region (1–60) of Exi-dimer compared with the control monomer (Fig. 6d). This result shows that the N-terminal regions are involved in exifone-induced dimerization of α-synuclein, in accordance with the results obtained from Asp-N digestion of the Exi-dimer. The gradual reduction in the signal intensities might be explained by heterogeneous dimerization around the N-terminus. The observed reduction in signal intensity, in our case, was not due to chemical exchange between the inhibitor-free and inhibitor-bound states of α-synuclein, as had been suggested by Rao *et al.*,[10] because the inhibitor-induced dimer and monomer were each purified to homogeneity and free or exchangeable inhibitors were removed by gel-filtration column chromatography and buffer exchange. Similar NMR spectra were observed for dopamine- and gossypetin-induced dimers (Supplementary Fig. S4), indicating that the N-terminal dimerization modes induced by dopamine, exifone, and gossypetin are the same or at least very similar. On the other hand, the C-terminal portion of exifone-bound dimer was still predominantly random coil in character, as observed in the control monomeric α-synuclein. These

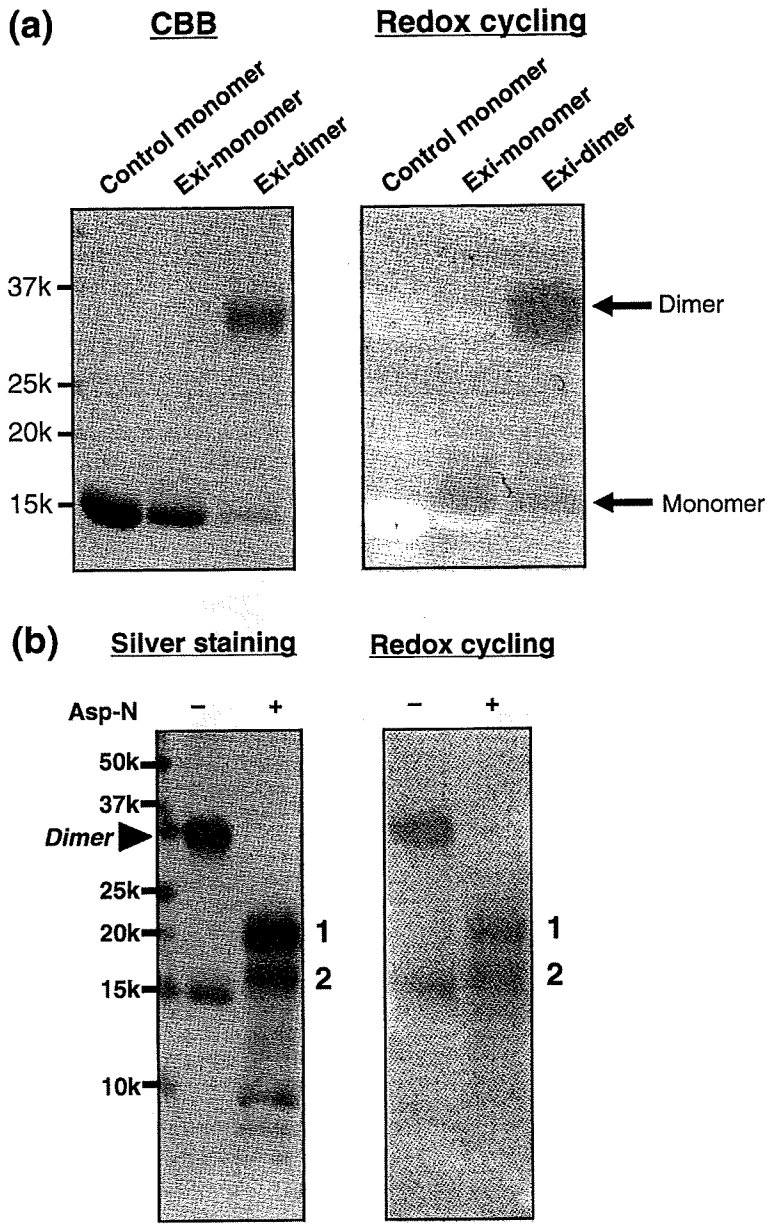

Fig. 4. Detection of exifone bound to α-synucleins by redox-cycling staining. (a) Control monomer, Exi-monomer, and Exi-dimer were stained with Coomassie brilliant blue (left) or by redox cycling (right). Exifone-bound α-synucleins were stained by redox cycling, appearing as purple-blue bands in the Exi-monomer and Exi-dimer lanes, due to NBT reduction to formazan (right). (b) Asp-N digestion of Exi-dimer. Exi-dimer was digested with endoproteinase Asp-N and the fragments were detected by silver staining (left) and redox staining (right). Two major bands corresponding to 20 kDa and 16 kDa (nos. 1 and 2, respectively) were positive for redox-cycling staining.

observations indicate the importance of the N-terminal region in α-synuclein assembly.

It is of note that three missense mutations in familial PD (A30P, E46K, and A53T) are located in the N-terminal region of α-synuclein. Recent NMR analyses suggest that these mutations may be altering the physicochemical properties of the protein, such as net charge (E46K) and secondary-structure propensity (A30P and A53T).[19] The binding of exifone, gossypetin, or dopamine to α-synuclein might also alter the net charge and/or secondary-structure propensity.

We did not observe the colloidal formation of exifone, gossypetin, or dopamine by electron microscopy (data not shown) as reported by Feng *et al.*[5] The discrepancy might be due to differences in the compounds used or differences in the proteins investigated. The inhibition mechanism of these three compounds seems rather specific because the N-terminal region was specifically involved in inhibitor binding, which is in contrast to the nonspecific colloidal inhibition.

In summary, we have characterized the inhibitor-bound α-synuclein dimer and showed that the N-terminal region (1–60) plays a key role in dimerization and inhibitor binding. Further studies are under way in our laboratory to elucidate the mechanisms of inhibitor-induced oligomer formation at atomic resolution.

Materials and Methods

Antibodies

Polyclonal antibodies were raised against synthetic peptides corresponding to residues 1–10, 11–20, 21–30, 31–40, 41–50, 51–60, 61–70, 75–91, and 131–140 of human α-synucleins, prepared as described previously.[12] Antibody

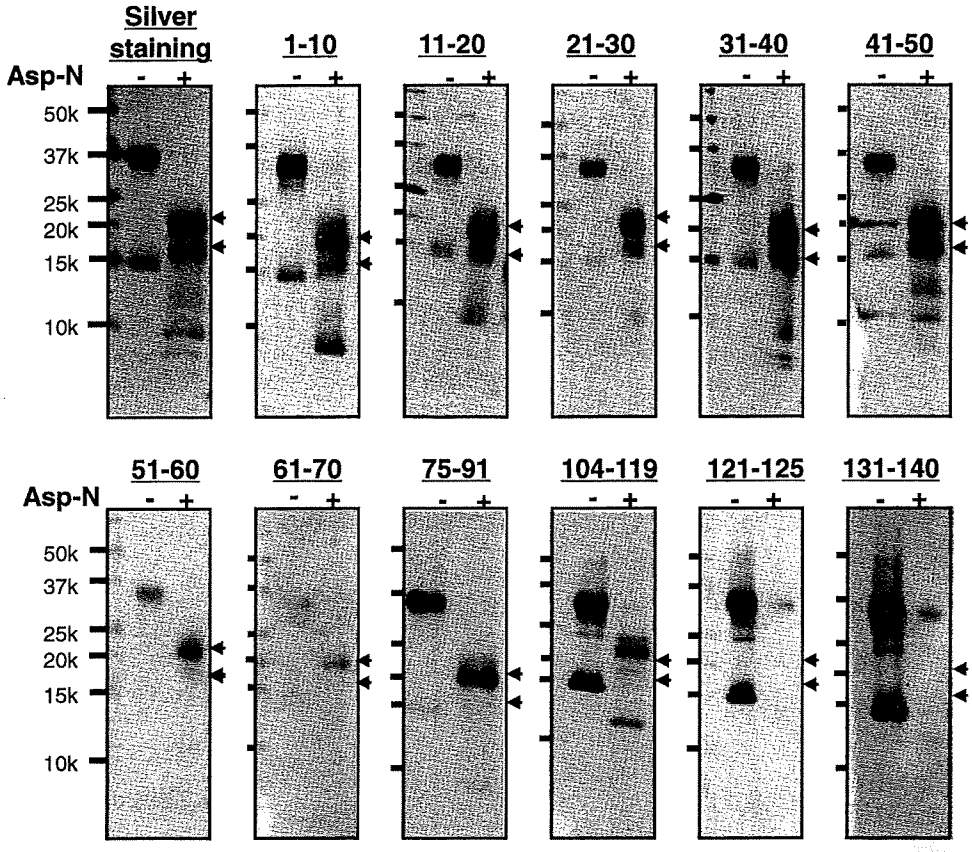

Fig. 5. Immunoblot analysis of Asp-N digests of Exi-dimer. Silver staining and immunoblots of Asp-N digests of Exi-dimer with a panel of anti-α-synuclein antibodies raised against nine peptides (corresponding to residues 1–10, 11–20, 21–30, 31–40, 41–50, 51–60, 61–70, 75–91, and 131–140).[12] Experimental details are given in Materials and Methods. Two major fragments (band nos. 1 and 2) were detected with silver staining (indicated with arrowheads). Fragment no. 1 was positive for antibodies to the N-terminal region, 1–97, and no. 2 was positive for antibodies to the N-terminal region, 1–50.

Syn259, which recognizes residues 104–119 of α-synuclein, was kindly provided by Dr. S. Nakajo. Monoclonal antibody Syn211, which recognizes residues 121–125 of α-synuclein, was purchased from Zymed.

Protein expression and purification

Expression of isotopically labeled α-synuclein was performed as described.[13] Human α-synuclein cDNA in bacterial expression plasmid pRK172 was used for production of isotopically labeled protein for NMR analyses.[20] Codon 136 was changed from TAC to TAT by site-directed mutagenesis to avoid cysteine misincorporation.[21] Uniformly ^{15}N-labeled α-synuclein was expressed in *Escherichia coli* BL21(DE3) cells grown in M9 minimal medium containing 1 g/L [^{15}N]NH_4Cl, while unlabeled α-synuclein was expressed using LB medium. Cell lysates were subjected to boiling and subsequently to ammonium sulfate precipitation. The precipitated α-synuclein was extensively dialyzed against 20 mM Tris–HCl (pH 8.0) and then purified with DEAE ion-exchange chromatography.

Preparation of inhibitor-bound α-synuclein monomers and dimers

Purified ^{15}N-labeled recombinant α-synuclein (9 mg/mL) was incubated with 2 mM inhibitor (exifone, gossypetin, or dopamine; see Fig. 1) for 30 days at 37 °C in 30 mM Tris–HCl containing 0.1% sodium azide. The samples were then centrifuged at 113,000*g* for 20 min. The supernatants were loaded on a Sephadex G-25 gel-filtration column to separate oligomers from unbound inhibitor. The eluates were fractionated on a Superdex 200 gel-filtration column (1 cm×30 cm), eluted with 10 mM Tris–HCl (pH 7.5) containing 150 mM NaCl. Eluates were monitored at 215 nm. α-Synuclein monomer and dimer fractions were each concentrated and the concentrates were subjected to NMR analysis. Protein concentrations were determined using HPLC and bicinchoninic acid protein assay kit (Pierce).

Mass spectrometry

Samples were spotted on a sample plate and mixed with the matrix solutions, saturated sinapic acid (Fluka) or α-cyano-4-hydroxycinnamic acid (Fluka) in 50% acetonitrile/H_2O containing 0.1% (v/v) trifluoroacetic acid. Mass spectra were obtained by MALDI-TOF MS using a Voyager-DE Pro mass spectrometer (PerSeptive Biosystems).

Peptide mapping of H_2O_2-treated and inhibitor-bound α-synucleins

Inhibitor-bound α-synuclein monomer and dimer were prepared as described above. For methionine oxidation, α-synuclein monomer (7 mg/mL) was incubated with 0–4% H_2O_2 at room temperature for 20 min and then dialyzed

against 30 mM Tris–HCl (pH 7.5) to remove H_2O_2. To identify the modification, inhibitor-bound α-synuclein monomer and dimer, as well as H_2O_2-treated α-synuclein, were incubated with trypsin at 37 °C for 18 h at an enzyme-to-substrate ratio of 1:50 (mol/mol) in 30 mM Tris–HCl (pH 7.5). Digested peptide products were separated by reverse-phase HPLC on a Supersphere Select B column (2.1 × 125 mm; Merck) and analyzed by MALDI-TOF MS.

Determination of stoichiometry of exifone/α-synuclein complexes

The stoichiometry of exifone/α-synuclein complexes was determined by measuring the absorbance of exifone at 385 nm using a spectrophotometer (UV-1600 PC, Shimadzu Co). Exifone-bound monomeric and dimeric α-synucleins were isolated by gel-filtration chromatography as described above.

Redox-cycle staining

Samples were subjected to SDS-PAGE and transferred onto polyvinylidene fluoride membranes. The membranes were incubated in 0.24 mM NBT (Sigma), 2 M potassium glycinate solution (pH 10.0) in the dark for 16 h at room temperature and then dipped in 100 mM sodium borate (pH 10.0). Exifone-bound α-synuclein was specifically stained as purple-blue bands due to NBT reduction to formazan.

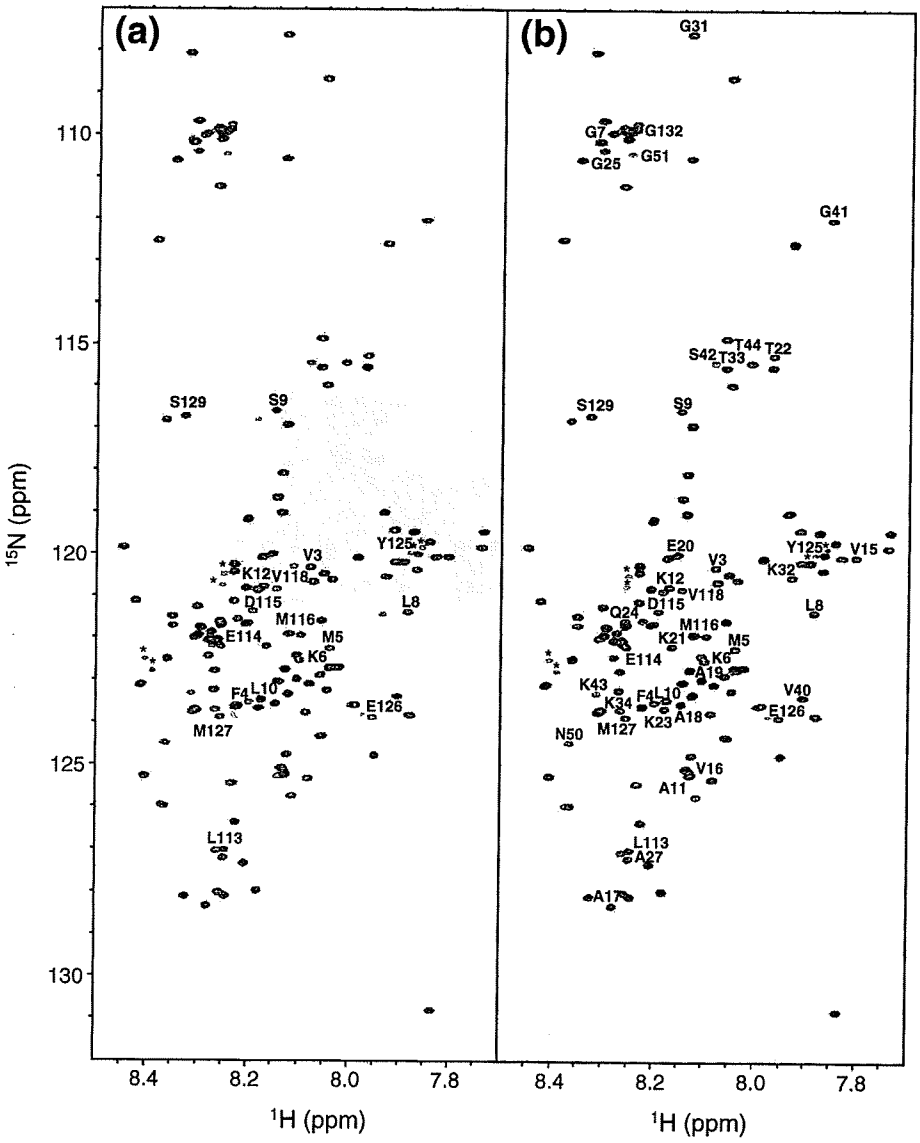

Fig. 6. NMR spectral comparison of exifone-bound ^{15}N-labeled α-synuclein dimer and control monomer. (a) ^{1}H–^{15}N HSQC spectra of ^{15}N-labeled Exi-monomer (red) and ^{15}N-labeled control monomer (black) recorded at a proton frequency of 920 MHz. (b) ^{1}H–^{15}N HSQC spectra of ^{15}N-labeled Exi-dimer (red) and ^{15}N-labeled control monomer (black). (c) Plot of the relative peak intensities, I(Exi-monomer)/I(monomer), of the HSQC cross-peaks in the Exi-monomer and control monomer *versus* the amino acid sequence of α-synuclein. (d) I(Exi-dimer)/I(monomer) of the HSQC cross-peaks in the Exi-dimer and control monomer. Signals derived from oxidized methionines and their neighboring residues (indicated with asterisks in a and b) were split and not taken into account. The peak splittings mostly reflect a mixture of *R* and *S* isomers of methionine sulfoxide.[18]

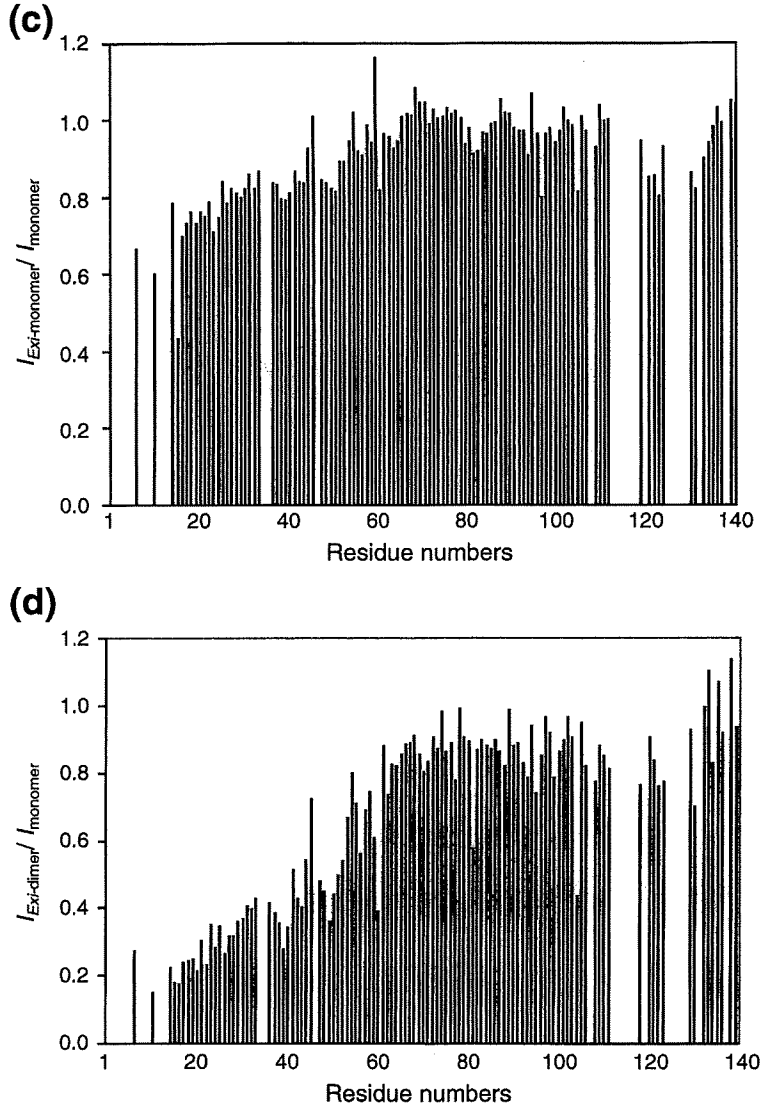

Fig. 6 *(legend on previous page)*

Asp-N digestion of α-synuclein dimer

α-Synuclein dimer (0.25 mg/mL) in 30 mM Tris–HCl (pH 7.5) was treated with 40 μg/mL of Asp-N (Roche) at 37 °C for 1 h. The reaction was stopped by adding 2× SDS sample buffer [4% SDS, 0.16 M Tris–HCl (pH 6.8), 30% glycerol] and the solution was boiled for 5 min. The samples were loaded onto 15% Tris/tricine SDS-PAGE gel, and the digested products were detected by silver staining (kit from Wako), immunoblotting, and redox-cycling staining. For immunoblotting, SDS-PAGE gels were blotted onto polyvinylidene fluoride membranes, blocked with 3% gelatin/phosphate-buffered saline, and incubated overnight at room temperature with anti-α-synuclein antibody in 10% FBS/phosphate-buffered saline. After washing, the blots were incubated for 2 h at room temperature with biotinylated secondary antibody (1:500) (Vector Laboratories). Following further washing, the blots were incubated with peroxidase-labeled avidin–biotin (Vector laboratories) for 30 min at room temperature and developed with $NiCl_2$-enhanced diaminobenzidine (Sigma).

NMR measurements

The samples for NMR experiments were prepared at a concentration of 0.1–1.0 mM in 90% H_2O/10% D_2O (v/v), 10 mM sodium phosphate buffer, and 100 mM NaCl at pH 7.0. NMR experiments were performed at 10 °C using a JEOL JNM-ECA920 spectrometer equipped with a 5-mm triple resonance probe. Backbone assignments of α-synuclein monomer were achieved by means of standard triple resonance experiments, as described previously.[13] The samples were checked by SDS-PAGE before and after NMR measurements, and it was confirmed that aggregation of inhibitor-bound α-synuclein monomer and dimer did not occur under these conditions. NMR time domain data were processed with the nmrPipe package[22] and the spectra were analyzed by using

Sparky software (T. D. Goddard and D. G. Kneller, University of California, San Francisco).

Acknowledgements

We thank K. Senda and K. Hattori (Nagoya City University) for help in the preparation of the recombinant proteins for NMR spectroscopy. We also thank M. Nakano (IMS) and T. Sugihara (JEOL) for help in NMR measurements and K. Matsumoto (RIKEN) for assistance in MS. We thank Drs. H. Sezaki, A. Hayashi, and T. Hosono (Agilent Technologies Japan) for their kind support in liquid chromatography–electrospray ionization MS analysis. This work was supported in part by Grants-in-Aid for Scientific Research on Priority Areas, Research on Pathomechanisms of Brain Disorders (to Y.Y., K.K., and M.H.), Grants-in-Aid for Scientific Research on Innovative Areas, Molecular Science of Fluctuations toward Biological Functions (to K.K.), and "Nanotechnology Network Project" of the Ministry of Education, Culture, Sports, Science and Technology (MEXT). This work was also supported by Takeda Science Foundation (Y.Y.).

Supplementary Data

Supplementary data associated with this article can be found, in the online version, at doi:10.1016/j.jmb.2009.10.068

References

1. Conway, K. A., Rochet, J. C., Bieganski, R. M. & Lansbury, P. T., Jr (2001). Kinetic stabilization of the α-synuclein protofibril by a dopamine-α-synuclein adduct. *Science*, **294**, 1346–1349.
2. Li, H. T., Lin, D. H., Luo, X. Y., Zhang, F., Ji, L. N., Du, H. N. *et al.* (2005). Inhibition of α-synuclein fibrillization by dopamine analogs via reaction with the amino groups of α-synuclein. Implication for dopaminergic neurodegeneration. *FEBS J.* **272**, 3661–3672.
3. Masuda, M., Suzuki, N., Taniguchi, S., Oikawa, T., Nonaka, T., Iwatsubo, T. *et al.* (2006). Small molecule inhibitors of α-synuclein filament assembly. *Biochemistry*, **45**, 6085–6094.
4. Porat, Y., Abramowitz, A. & Gazit, E. (2006). Inhibition of amyloid fibril formation by polyphenols: structural similarity and aromatic interactions as a common inhibition mechanism. *Chem. Biol. Drug Des.* **67**, 27–37.
5. Feng, B. Y., Toyama, B. H., Wille, H., Colby, D. W., Collins, S. R., May, B. C. *et al.* (2008). Small-molecule aggregates inhibit amyloid polymerization. *Nat. Chem. Biol.* **4**, 197–199.
6. Norris, E. H., Giasson, B. I., Hodara, R., Xu, S., Trojanowski, J. Q., Ischiropoulos, H. & Lee, V. M. (2005). Reversible inhibition of α-synuclein fibrillization by dopaminochrome-mediated conformational alterations. *J. Biol. Chem.* **280**, 21212–21219.
7. Herrera, F. E., Chesi, A., Paleologou, K. E., Schmid, A., Munoz, A., Vendruscolo, M. *et al.* (2008). Inhibition of α-synuclein fibrillization by dopamine is mediated by interactions with five C-terminal residues and with E83 in the NAC region. *PLoS ONE*, **e3394**, 3.
8. Ehrnhoefer, D. E., Bieschke, J., Boeddrich, A., Herbst, M., Masino, L., Lurz, R. *et al.* (2008). EGCG redirects amyloidogenic polypeptides into unstructured, off-pathway oligomers. *Nat. Struct. Mol. Biol.* **15**, 558–566.
9. Moussa, C. E., Mahmoodian, F., Tomita, Y. & Sidhu, A. (2008). Dopamine differentially induces aggregation of A53T mutant and wild type α-synuclein: insights into the protein chemistry of Parkinson's disease. *Biochem. Biophys. Res. Commun.* **365**, 833–839.
10. Rao, J. N., Dua, V. & Ulmer, T. S. (2008). Characterization of α-synuclein interactions with selected aggregation-inhibiting small molecules. *Biochemistry*, **47**, 4651–4656.
11. Hong, D. P., Fink, A. L. & Uversky, V. N. (2008). Structural characteristics of α-synuclein oligomers stabilized by the flavonoid baicalein. *J. Mol. Biol.* **383**, 214–223.
12. Masuda, M., Hasegawa, M., Nonaka, T., Oikawa, T., Yonetani, M., Yamaguchi, Y. *et al.* (2009). Inhibition of α-synuclein fibril assembly by small molecules: analysis using epitope-specific antibodies. *FEBS Lett.* **583**, 787–791.
13. Sasakawa, H., Sakata, E., Yamaguchi, Y., Masuda, M., Mori, T., Kurimoto, E. *et al.* (2007). Ultra-high field NMR studies of antibody binding and site-specific phosphorylation of α-synuclein. *Biochem. Biophys. Res. Commun.* **363**, 795–799.
14. Uversky, V. N., Yamin, G., Souillac, P. O., Goers, J., Glaser, C. B. & Fink, A. L. (2002). Methionine oxidation inhibits fibrillation of human α-synuclein *in vitro*. *FEBS Lett.* **517**, 239–244.
15. Paz, M. A., Gallop, P. M., Torrelio, B. M. & Fluckiger, R. (1988). The amplified detection of free and bound methoxatin (PQQ) with nitroblue tetrazolium redox reactions: insights into the PQQ-locus. *Biochem. Biophys. Res. Commun.* **154**, 1330–1337.
16. Ingrosso, D., Fowler, A. V., Bleibaum, J. & Clarke, S. (1989). Specificity of endoproteinase Asp-N (Pseudomonas fragi): cleavage at glutamyl residues in two proteins. *Biochem. Biophys. Res. Commun.* **162**, 1528–1534.
17. Tetaz, T., Morrison, J. R., Andreou, J. & Fidge, N. H. (1990). Relaxed specificity of endoproteinase Asp-N: this enzyme cleaves at peptide bonds N-terminal to glutamate as well as aspartate and cysteic acid residues. *Biochem. Int.* **22**, 561–566.
18. Stadtman, E. R., Van Remmen, H., Richardson, A., Wehr, N. B. & Levine, R. L. (2005). Methionine oxidation and aging. *Biochim. Biophys. Acta*, **1703**, 135–140.
19. Rospigliosi, C. C., McClendon, S., Schmid, A. W., Ramlall, T. F., Barre, P., Lashuel, H. A. & Eliezer, D. (2009). E46K Parkinson's-linked mutation enhances C-terminal-to-N-terminal contacts in α-synuclein. *J. Mol. Biol.* **388**, 1022–1032.
20. Jakes, R., Spillantini, M. G. & Goedert, M. (1994). Identification of two distinct synucleins from human brain. *FEBS Lett.* **345**, 27–32.
21. Masuda, M., Dohmae, N., Nonaka, T., Oikawa, T., Hisanaga, S., Goedert, M. & Hasegawa, M. (2006). Cysteine misincorporation in bacterially expressed human α-synuclein. *FEBS Lett.* **580**, 1775–1779.
22. Delaglio, F., Grzesiek, S., Vuister, G. W., Zhu, G., Pfeifer, J. & Bax, A. (1995). NMRPipe: a multidimensional spectral processing system based on UNIX pipes. *J. Biomol. NMR*, **6**, 277–293.

THE JOURNAL OF BIOLOGICAL CHEMISTRY VOL. 284, NO. 12, pp. 7940–7950, March 20, 2009

Conversion of Wild-type α-Synuclein into Mutant-type Fibrils and Its Propagation in the Presence of A30P Mutant*[S]

Received for publication, September 26, 2008, and in revised form, January 21, 2009 Published, JBC Papers in Press, January 21, 2009, DOI 10.1074/jbc.M807482200

Motokuni Yonetani[‡§], Takashi Nonaka[‡], Masami Masuda[‡§], Yuki Inukai[‡§], Takayuki Oikawa[‡§], Shin-ichi Hisanaga[§], and Masato Hasegawa[‡1]

From the [‡]Department of Molecular Neurobiology, Tokyo Institute of Psychiatry, 2-1-8 Kamikitazawa, Setagaya-ku, 156-8585 Tokyo, Japan and the [§]Molecular Neuroscience Laboratory, Graduate School of Science and Engineering, Tokyo Metropolitan University, 1-1 Minami-Osawa, Hachioji-shi, 192-0397 Tokyo, Japan

Fibrillization or conformational change of α-synuclein is central in the pathogenesis of α-synucleinopathies, such as Parkinson disease. We found that the A30P mutant accelerates nucleation-dependent fibrillization of wild type (WT) α-synuclein. Electron microscopy observation and ultracentrifugation experiments revealed that shedding of fragments occurs from A30P fibrils and that these fragments accelerate fibrillization by serving as seeds. Immunochemical analysis using epitope-specific antibodies and biochemical analyses of protease-resistant cores demonstrated that A30P fibrils have a distinct conformation. Interestingly, WT fibrils formed with A30P seeds exhibited the same character as A30P fibrils, as did A30P fibrils formed with WT seeds, indicating that the A30P mutation affects the conformation and fibrillization of both WT and A30P. These effects of A30P mutation may explain the apparent conflict between the association of A30P with Parkinson disease and the slow fibrillization of A30P itself and therefore provide new insight into the molecular mechanisms of α-synucleinopathies.

Parkinson disease (PD)[2] is the second most common neurodegenerative disorder, after Alzheimer disease. Neuropathological features of PD are selective loss of dopaminergic neurons in the substantia nigra and appearance of intracellular inclusion bodies, referred to as Lewy bodies (LBs) and Lewy neurites. Ultrastructurally, LBs are composed of a dense core of filamentous and granular material that is surrounded by radially oriented fibrils (1, 2). Biochemical and immunochemical analyses showed that hyperphosphorylated α-synuclein is the major component of the fibrous structures of LBs and Lewy neurites (3).

Genetic analyses of α-synuclein gene of familial cases of PD and dementia with LBs have demonstrated that expression of abnormal α-synuclein or overexpression of normal α-synuclein is associated with these diseases; namely, three missense mutations (A53T (4), A30P (5), and E46K (6)) and multiplication (7–12) of the α-synuclein gene have been found to cosegregate with the onset of PD in kindreds of autosomal dominantly inherited familial PD and dementia with LBs.

α-Synuclein is a 140-amino acid protein, harboring seven imperfect tandem repeats (KTKEGV-type) in the N-terminal half, followed by a hydrophobic central region (non-Aβ component of Alzheimer disease (NAC)) and an acidic C-terminal. The tandem repeat region has been assumed to form an amphipathic α-helix by binding to phospholipid (13). Circular dichroism and Fourier-transform IR analysis revealed that α-synuclein is a natively unfolded protein with little ordered secondary structure (14). However, recent NMR analyses have revealed three intramolecular long range interactions. These interactions are between the highly hydrophobic NAC region (residues 85–95) and the C terminus (residues 110–130), C-terminal residues 120–130 and residues 105–115, and the region around residue 120 and the N terminus around residue 20 (15).

Recombinant α-synuclein *in vitro* assembles into fibrils that closely resemble those in brains with PD and dementia with LBs upon incubation at a high concentration at 37 °C with shaking, whereas other synuclein family proteins (*i.e.* β-synuclein and γ-synuclein) neither accumulate in the brain (1, 16) nor form fibrils (17–19). During the assembly of α-synuclein fibrils, conformational change from random coil to β-sheet structure can be observed. It has been shown that the sequence of the NAC region in α-synuclein is necessary for the assembly (20).

Mostly in *in vitro* experiments, it has been shown that the A53T and E46K mutations promote fibrillization (17, 21–25), whereas the effect of A30P mutation on fibrillization is unclear. It has been reported that A30P mutation promotes oligomerization of nonfibrillar protofibrils (23, 26) and that some of the protofibrils with a circular morphology may form pores by binding to ER membrane (27). It has also been reported that A30P mutation is defective in binding to phospholipid vesicles, and the alteration of membrane interaction could contribute to early onset of PD (28, 29).

* This work was supported by a Grant-in-Aid for Scientific Research on Priority Areas, Research on Pathomechanisms of Brain Disorders (to M. H.), a Grant-in-Aid for Scientific Research (B) (to M. H.), and a Grant-in-Aid for Scientific Research (C) (to M. H.) from the Ministry of Education, Culture, Sports, Science and Technology of Japan. The costs of publication of this article were defrayed in part by the payment of page charges. This article must therefore be hereby marked "*advertisement*" in accordance with 18 U.S.C. Section 1734 solely to indicate this fact.

[S] The on-line version of this article (available at http://www.jbc.org) contains supplemental Figs. 1–3.

[1] To whom correspondence should be addressed: Dept. of Molecular Neurobiology, Tokyo Institute of Psychiatry, Tokyo Metropolitan Organization for Medical Research, 2-1-8 Kamikitazawa, Setagaya-ku, Tokyo 156-8585, Japan. Tel.: 81-3-3304-5701; Fax: 81-3-3329-8035; E-mail: masato@prit.go.jp.

[2] The abbreviations used are: PD, Parkinson disease; LB, Lewy body; WT, wild type; NAC, non-Aβ component of Alzheimer disease; Th-S, thioflavin S; MOPS, 3-(*N*-morpholino)propanesulfonic acid; CBB, Coomassie Brilliant Blue; MTT, 3-(4,5-dimethylthiazol-2-yl)-2,5-diphenyltetrazolium bromide; EM, electron microscopy.

Assembly of protein into fibrils is usually a nucleation-dependent process that consists of a lag phase (nucleation) and a growth phase (elongation). α-Synuclein fibrillization was confirmed to be a nucleation-dependent process (22). The addition of seeds to the monomer promotes fibrillization by rendering the nucleation process redundant. Not only wild type (WT) fibrils but also A53T fibrils have been reported to act as nuclei for fibrillization of WT α-synuclein (30).

In this study, we have investigated nucleation-dependent fibrillization of WT and A30P α-synuclein and the conformations of WT and A30P fibrils formed in the presence of WT and A30P seeds. We found that A30P seeds accelerated the nucleation-dependent fibrillization of WT α-synuclein more effectively than did WT seeds. Further, A30P fibrils have a distinct conformation from WT fibrils and show a higher level of fragment shedding. The WT fibrils formed in the presence of A30P seeds showed the same character as A30P fibrils, suggesting that the nucleation-dependent assembly of WT fibrils in the presence of A30P seeds results in conversion of WT conformation to that of A30P. Further, the A30P fibrils formed in the presence of WT seeds shared the properties of A30P fibrils. The *in vitro* results shown here implicate the structural and functional differences among α-synuclein amyloid fibrils, useful for understanding the pathogenesis of α-synucleinopathies.

EXPERIMENTAL PROCEDURES

Antibodies—α-Synuclein epitope-specific polyclonal antibodies syn1–10, syn75–91, and syn131–140 were raised against synthetic peptides MDVFMKGLSKC (residues 1–10 with Cys at the C terminus), CTAVAQKTVEGAGSIAAA (residues 75–91 with Cys at the N terminus), and CEGYQDYEPEA (residues 131–140 with Cys at the N terminus) of human α-synuclein, respectively. Peptides were conjugated to *m*-maleimidobenzoyl-*N*-hydrosuccinimide ester-activated keyhole limpet hemocyanin. The keyhole limpet hemocyanin-peptide complex (1 mg of each immunogen) emulsified in Freund's complete adjuvant was injected subcutaneously into a New Zealand white rabbit, followed by five weekly subcutaneous injections of 150 mg of KLH-peptide complex emulsified in Freund's incomplete adjuvant starting from 3 weeks after the first immunization. Other anti-α-synuclein antibodies, number 36 (residues 1–10) and NAC2 (residues 75–91), were kindly provided by Dr. Iwatsubo and Dr. Jäkälä, respectively.

Expression and Purification of Human WT and Mutant α-Synuclein—Human α-synuclein cDNA in bacterial expression plasmid pRK172 was provided by Dr. Goedert. A30P, E46K, and A53T mutations were induced by site-directed mutagenesis (Stratagene). WT and mutant α-synuclein were expressed in *Escherichia coli* BL21 (DE3) cells and purified as described (31). Protein concentration was determined as described (31).

Fibrillization of WT and Mutant α-Synuclein—Purified WT and mutant α-synuclein (1 mg/ml) were each incubated at 37 °C, with shaking at 200 rpm in 30 mM Tris-HCl, pH 7.5, containing 0.1% NaN_3. For quantitative assessment of fibrillization, aliquots (10 μl) of assembly mixture were removed at various time points, brought to 300 μl with 5 mM Thioflavin S (Th-S) in 20 mM MOPS, pH 6.8, and incubated for 60 min at room temperature. Fluorimetry was performed using a Hitachi F4000 fluorescence spectrophotometer (set at 440 nm excitation/521 nm emission) as described (32).

Preparation of Seeds—Purified WT and mutant α-synuclein (7 mg/ml) were each incubated for 96–120 h at 37 °C, with shaking at 200 rpm in 30 mM Tris-HCl, pH 7.5, containing 0.1% NaN_3. Assembly mixture was diluted in 5 volumes of 30 mM Tris-HCl, pH 7.5, and ultracentrifuged at 151,000 × *g* for 20 min at 25 °C. The pellets were resuspended in 5 volumes of 30 mM Tris-HCl, pH 7.5, and ultracentrifuged at 151,000 × *g* for 20 min again. The pellets were resuspended homogeneously by pipetting in 30 mM Tris-HCl, pH 7.5, containing 0.1% NaN_3 and used as seeds. Aliquots of seeds or fibrils were solubilized in 6 M guanidine hydrochloride, and the concentration of α-synuclein was determined as described (31).

Nucleation-dependent Fibrillization of α-Synuclein—Purified WT or mutant α-synuclein (1 mg/ml) in 30 mM Tris-HCl, pH 7.5, containing 0.1% NaN_3 was incubated with seeds (1% of total protein) for 0–144 h at 37 °C without shaking. Fibrillization was monitored by measuring Th-S fluorescence.

Semiquantitative Analysis of Fibril Length in Suspended Fibrils—Fibrils formed in the presence or absence of seeds (0.1 mg/ml) were observed at a magnification of ×25,000 by electron microscopy after suspension by pipetting. Fibril length was measured on the photographs, and the populations were calculated.

Characterization of Seeds by Ultracentrifugation—Seeds or fibrils formed in the presence of seeds (1.0 mg/ml) were suspended in 5 volumes of 30 mM Tris-HCl, pH 7.5, and incubated for 30 min at room temperature, followed by ultracentrifugation for 20 min at 109,000 × *g*. The pellets were resuspended in equal volumes of the supernatant with 30 mM Tris-HCl, pH 7.5. The supernatant and suspension were treated with 5× SDS sample buffer and subjected to SDS-PAGE. After staining of gels with Coomassie Brilliant Blue (CBB) and scanning, the intensities of the α-synuclein band were quantified by Scion Image (Scion Corp.). Aliquots of the supernatants were examined by electron microscopy and used for studies of nucleation-dependent fibrillization.

Electron Microscopy—Fibrils, seeds and fibrils formed in the presence of seeds were diluted in 30 mM Tris-HCl, pH 7.5. Aliquots of these dilutions and centrifugal supernatants of seeds and fibrils formed in the presence of seeds were placed on 400-mesh collodion-coated grids, negatively stained with 2% lithium phosphotungstate, and observed with a JEOL 1200EXII electron microscope.

Dot Blot Assay—α-Synuclein monomer, seeds and fibrils formed in the presence of seeds were diluted in 30 mM Tris-HCl, pH 7.5, 0.1% NaN_3 and spotted onto polyvinylidene difluoride membrane. The membrane was probed with epitope-specific α-synuclein antibodies syn1–10 (N-terminal region), syn75–91 (NAC region), and syn131–140 (C-terminal region) or stained with CBB to detect total protein. Immunoreactivity was visualized using the avidin-biotin detection system (Vector Laboratories) and quantified by scanning as described above.

Comparison of Protease-resistant Cores of α-Synuclein Fibrils—Seeds or fibrils formed in the presence of seeds (1.0 mg/ml) were sonicated and treated with 50 μg/ml trypsin or 2 μg/ml

Effect of A30P Mutation on Fibrillization of α-Synuclein

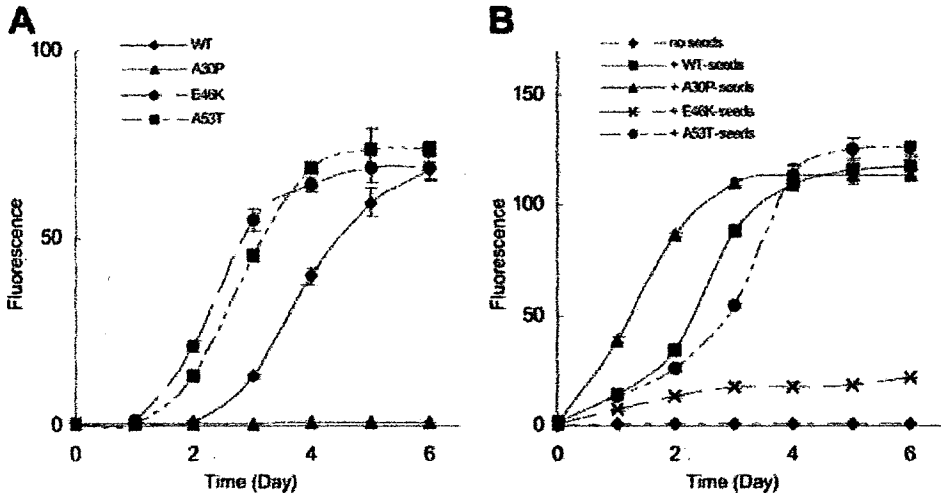

FIGURE 1. **Fibrillization of WT and mutant α-synuclein (*A*) and promotion of WT α-synuclein fibrillization by the addition of WT or mutant fibrils seeds (*B*).** *A*, WT and mutant α-synuclein (1.0 mg/ml) were incubated with shaking at 37 °C in the absence of seeds. *B*, WT α-synuclein (1.0 mg/ml) was incubated without shaking at 37 °C in the presence of WT or mutant fibril seeds (0.1% of total protein). Fibrillization was monitored by measuring the Th-S fluorescence. Results are expressed as means ± S.E. ($n = 3$).

proteinase K at 37 °C for 30 min. The reaction was stopped by boiling for 5 min. The solution was treated with sample buffer containing 2% SDS and 8 M urea and subjected to SDS-PAGE.

Cytotoxicity Assay—The cytotoxic effect of α-synuclein fibrils was assessed by measuring cellular redox activity with 3-(4,5-dimethylthiazol-2-yl)-2,5-diphenyltetrazolium bromide (MTT), as described (33). Briefly, SH-SY5Y cells cultured in a 96-well microtiter plate were treated with 500 nM α-synuclein monomer, fibrils (suspended by pipetting or sonication), or fibrils formed in the presence of seeds. Following a 6-h incubation, the cytotoxic effect was assessed by measuring cellular redox activity.

Statistical Analysis—Statistic analysis was performed using unpaired Student's *t* test. The results are expressed as means ± S.E. of three independent experiments ($n = 3$).

RESULTS

Effect of A30P Seeds on Fibrillization of α-Synuclein—First, we tested the effect of mutations on fibrillization of α-synuclein. As shown in Fig. 1*A*, both A53T and E46K mutants fibrillized faster than WT, whereas the fibrillization of A30P mutant was much slower than that of WT, confirming the previous observations. Since A53T fibrils can act as seeds for the fibrillization of WT α-synuclein (30), we next investigated whether A30P fibrils also act as seeds for WT monomer. We incubated WT α-synuclein with WT, A30P, E46K, or A53T seeds under conditions where WT α-synuclein itself does not form fibrils and analyzed fibrillization (Fig. 1*B*). Fibrillization was observed following the addition of either WT seeds or mutant seeds. Interestingly, the assembly was faster in the presence of A30P seeds than in the presence of WT or the other mutant seeds. The time required for half-maximal fibrillization was ~1.5 days with A30P seeds, which is shorter than those with the other seeds, WT (2.5 days), E46K (more than 6 days), and A53T (6 days).

In the brains of patients with the A30P mutation, both WT and A30P α-synuclein are expressed. Therefore, a mixture of WT and A30P α-synuclein was incubated with WT or A30P seeds, and the progress of fibrillization was observed in terms of Th-S fluorescence intensity. As in the case of WT α-synuclein monomer alone, A30P seeds accelerated the fibrillization process more effectively than did WT seeds (supplemental Fig. 1). Fibrillization was not observed in the absence of seeds. The time for half-maximal fibrillization was ~1.5 days with A30P seeds and 3.5 days with WT seeds.

Shedding of Fragments from A30P Fibrils—To elucidate the mechanism of the effect of A30P seeds on fibrillization, we utilized electron microscopy (Fig. 2). Many tiny or short fibrils were observed in A30P seeds, whereas relatively long fibrils were predominantly detected in WT, E46K, and A53T seeds (Fig. 2*A*, *v*, *vi*, *vii*, and *viii*). This observation was confirmed by measuring the fibril length in these seeds. Short fibrils of less than 100 nm were predominant in the A30P seeds, whereas longer fibrils were detected in the WT and A53T seeds (supplemental Fig. 3*A*). Before preparation of the seeds, WT and mutant α-synuclein fibrils were uniformly long and showed no morphological differences (Fig. 2*A*, *i*, *ii*, *iii*, and *iv*). Therefore, it appeared that A30P fibrils readily fragmented during the process of seed preparation. To test whether the small fibrils could be separated by centrifugation or not, WT and mutant α-synuclein seeds were ultracentrifuged, and the supernatants were observed by electron microscopy. Surprisingly, many tiny fibrils were observed in the supernatant of A30P seeds, whereas such tiny fibrils were hardly detected in the supernatant of WT, E46K, and A53T seeds (Fig. 2*A*, *ix*, *x*, *xi*, and *xii*), indicating that A30P fibrils have a higher propensity for shedding fragments than do WT fibrils and that the small fragments are recovered in the supernatant of ultracentrifugation.

We then attempted to quantitate the fragmented fibrils by ultracentrifugation. The centrifugal supernatant was subjected to SDS-PAGE, and the gel was stained with CBB. As expected, more α-synuclein was detected in the supernatant of A30P seeds than in those of WT, E46K, and A53T seeds (Fig. 2, *B* and *C*).

Next, we investigated whether the tiny fibrils recovered in the supernatant of ultracentrifugation can act as seeds for fibrillization of α-synuclein. WT α-synuclein was incubated with the supernatant of WT, A30P, E46K, or A53T seeds (10% of total volume), and fibrillization was monitored by a Th-S assay. In the presence of the supernatant of WT, E46K, and A53T seeds, a very slow increase of Th-S was observed, whereas fibrillization was accelerated in the presence of the supernatant of A30P seeds (Fig. 2*D*), as seen in the fibrillization in Fig. 1*B*. These results indicate that the A30P fibrils readily shed many tiny fibrils that can act as seeds for fibrillization.

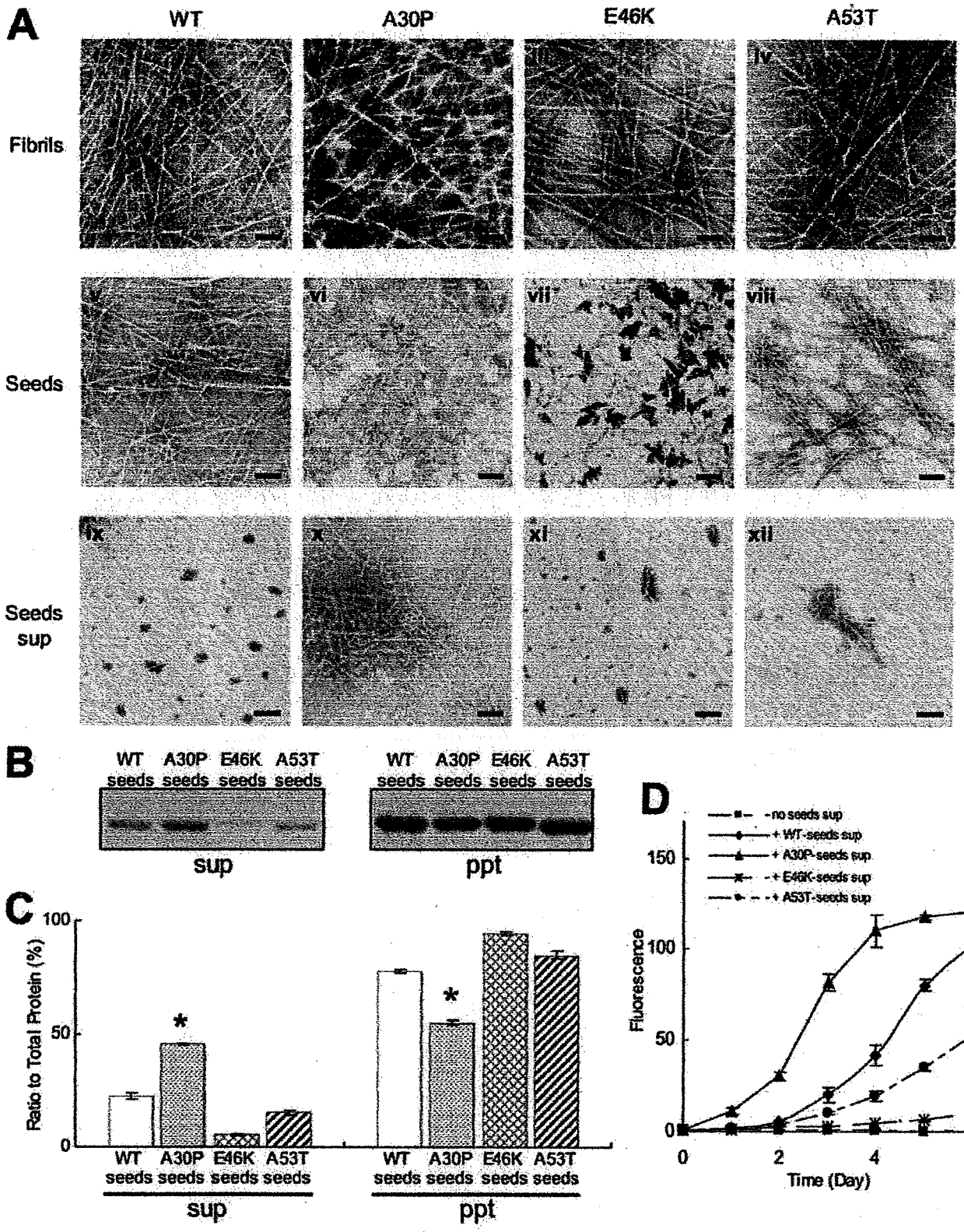

FIGURE 2. **EM and biochemical analyses of WT and mutant seeds.** *A*, electron microscopy of WT and mutant fibrils, fibril seeds, and seed supernatants (*sup*) after ultracentrifugation. Shown are fibrils (*i*, *ii*, *iii*, and *iv*), seeds (*v*, *vi*, *vii*, and *viii*), and seed supernatants (*ix*, *x*, *xi*, and *xii*) of WT (*i*, *v*, and *ix*), A30P (*ii*, *vi*, and *x*), E46K (*iii*, *vii*, and *xi*), and A53T (*iv*, *viii*, and *xii*) α-synuclein. Negatively stained fibrils, seeds, or seed supernatants were observed by electron microscopy. *Scale bar*, 200 nm. *B*, biochemical analysis of WT and mutant seeds after ultracentrifugation. Pellets and supernatants were subjected to SDS-PAGE and stained with CBB. *C*, quantification of α-synuclein recovered in the supernatants and pellets (expressed as a percentage of total α-synuclein, taken as 100%). The results are expressed as means ± S.E. ($n = 3$) (*, $p < 0.01$). *D*, WT α-synuclein monomer seeding activities of short fibrils recovered in the supernatants of ultracentrifugation. The results are expressed as means ± S.E. ($n = 3$).

Effect of A30P Mutation on Fibrillization of α-Synuclein

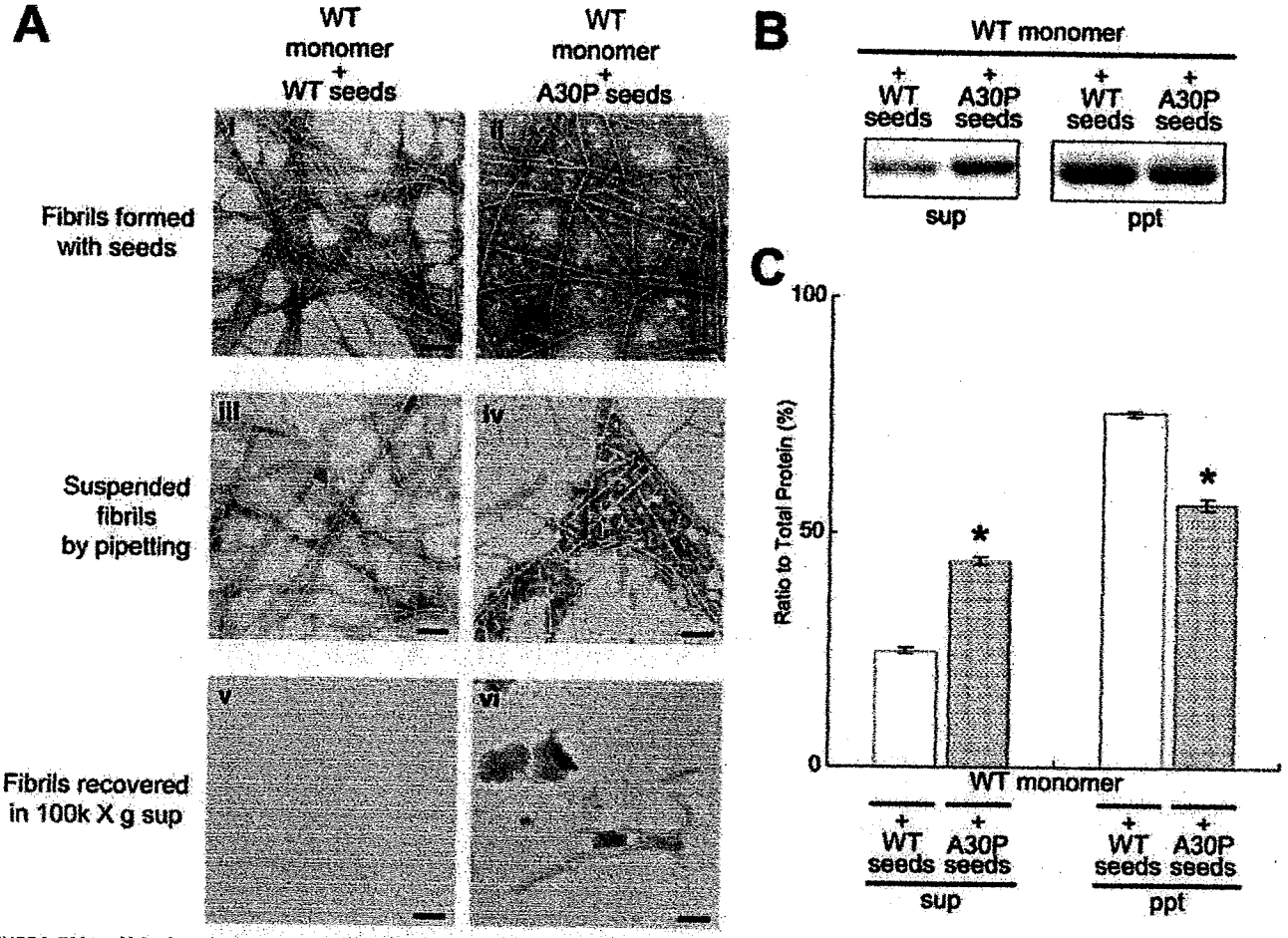

FIGURE 3. **EM and biochemical analyses of WT fibrils formed in the presence of WT or A30P seeds.** *A*, EM analysis of WT fibrils formed in the presence of WT or A30P seeds, suspended fibrils, and the supernatants after ultracentrifugation for WT fibrils formed with WT seeds (*i*, *iii*, and *v*) and WT fibrils formed with A30P seeds (*ii*, *iv*, and *vi*). Negatively stained WT fibrils formed in the presence of WT or A30P seeds (*i* and *ii*), the fibrils after suspension (*iii* and *iv*), and the fibrils in the supernatants after centrifugation (*iv* and *v*) were observed by electron microscopy. *Scale bar*, 200 nm. *B*, biochemical analysis of α-synuclein fibrils fractionated by ultracentrifugation. *C*, quantification of α-synuclein recovered in the supernatants and pellets after ultracentrifugation (expressed as a percentage of total α-synuclein, taken as 100%). The results are expressed as means ± S.E. ($n = 3$) (*, $p < 0.01$).

Shedding Property of WT Fibrils Formed in the Presence of A30P Seeds—Next, we investigated whether or not the WT fibrils formed in the presence of A30P seeds have the same properties as A30P fibrils (Fig. 3*A*). The WT fibrils formed in the presence of A30P seeds appeared to be morphologically indistinguishable from the WT fibrils formed in the presence of WT seeds before preparation of suspensions (Fig. 3*A*, *i* and *ii*). However, after suspension, many tiny fibrils were shed from WT fibrils formed in the presence of A30P seeds, whereas only a few short fibrils were shed from WT fibrils formed in the presence of WT seeds (Fig. 3*A*, *iii* and *iv*). This was confirmed by measuring the fibril length in these suspensions of fibrils produced by pipetting (supplemental Fig. 3*B*). After ultracentrifugation, many tiny fibrils were observed in the supernatant of WT fibrils formed in the presence of A30P seeds, whereas few such fibrils were detected in the supernatant of WT fibrils formed in the presence of WT seeds (Fig. 3*A*, *v* and *vi*). Quantitative analysis confirmed that a larger amount of α-synuclein was present in the supernatant of WT fibrils formed in the presence of A30P seeds than in that of WT fibrils formed in the presence of WT seeds (Fig. 3, *B* and *C*). These results suggest that WT fibrils formed in the presence of A30P seeds have the same shedding propensity as A30P fibrils.

Immunochemical Analysis of α-Synuclein Fibrils with Epitope-specific Antibodies—To investigate the structural differences between WT fibrils and A30P fibrils and between WT fibrils formed in the presence of WT seeds and WT fibrils formed in the presence of A30P seeds, we employed a dot blot assay with three epitope-specific antibodies to α-synuclein, syn1–10 (N-terminal region), syn75–91 (NAC region), and syn131–140 (C-terminal region).

As shown in Fig. 4, *G* and *I*, syn131–140 stained both WT and A30P fibrils (fibril seeds) almost equally, whereas syn75–91 (Fig. 4, *E* and *I*) strongly labeled only WT fibrils. syn1–10 (Fig. 4, *C* and *I*) labeled A30P fibrils more strongly than WT fibrils. Similar results were obtained with other independently produced anti-α-synuclein antibodies to the N terminus (number 36, a gift from Dr. Iwatsubo) and anti-NAC antibody (NAC2, a gift form Dr. Jäkälä) (data not shown). These results suggest that the conformation of A30P fibrils is different from that of WT fibrils. Interestingly, dot blot analysis of WT fibrils formed in the presence of A30P seeds showed a pattern of immunore-

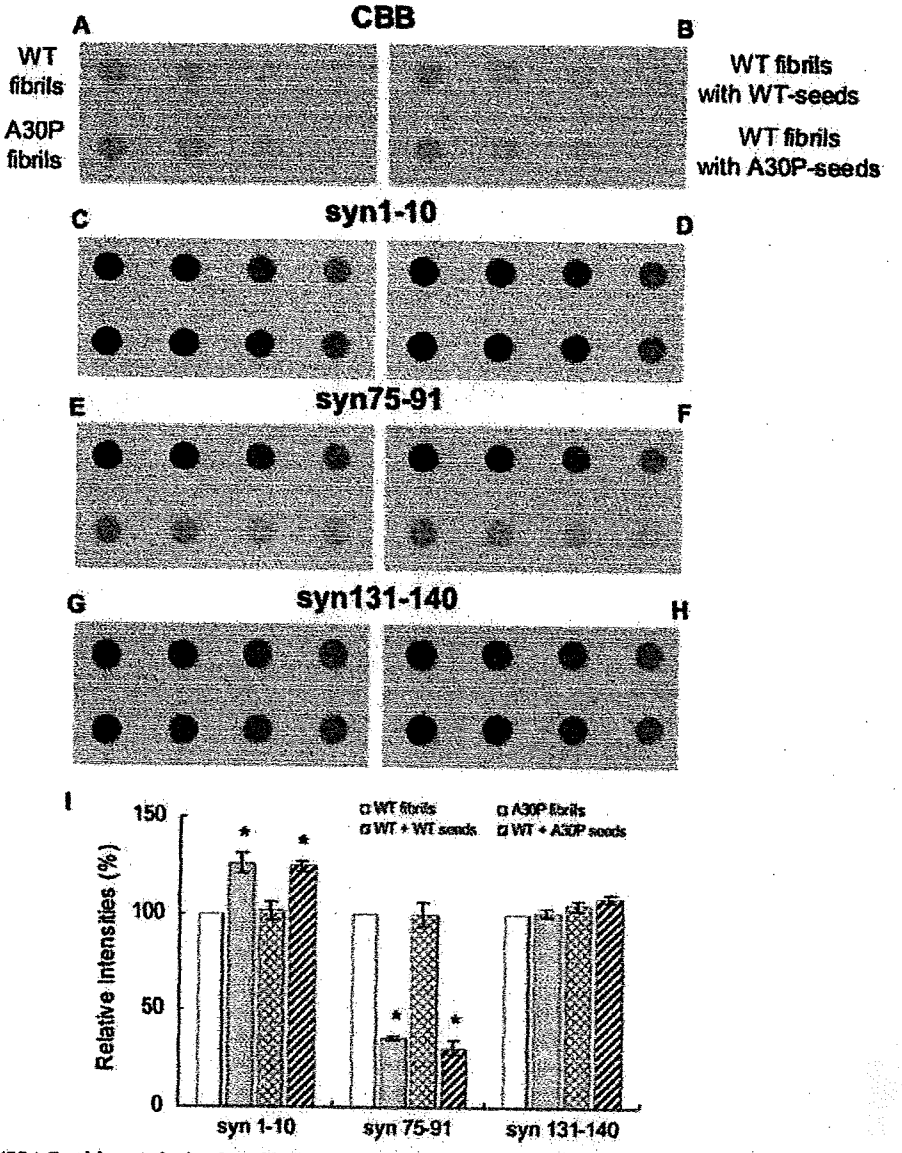

FIGURE 4. **Dot blot analysis of WT fibrils formed in the presence of A30P fibril seeds with epitope-specific antibodies.** Equal amounts of serially diluted WT fibrils, A30P fibrils, WT fibrils formed in the presence of WT seeds, and WT fibrils formed in the presence of A30P seeds were spotted onto polyvinylidene difluoride membrane, stained with CBB (*A* and *B*), or immunodetected with syn1–10 (*C* and *D*), syn75–91 (*E* and *F*), and syn131–140 antibodies (*G* and *H*). For CBB staining and dot blotting with syn74–91, 100, 50, 25, and 12.5 ng of protein were spotted. For immunodetection with syn1–10 and syn131–140, 10, 5, 2.5, and 1.25 ng of protein were spotted. A typical experiment is shown; similar results were obtained in three separate experiments. *I*, quantification of immunoreactivities of WT fibrils, A30P fibrils, and WT fibrils formed in the presence of WT seeds or A30P seeds. The results are expressed as a percentage of immunoreactivity of WT fibrils, taken as 100% (means ± S.E., $n = 3$) (*, $p < 0.01$).

activity similar to that of A30P fibrils (Fig. 4, *D*, *F*, and *I*), whereas WT fibrils formed in the presence of WT seeds showed the same pattern as WT fibrils (Fig. 4, *D*, *F*, and *I*). These results suggest that the WT fibrils formed in the presence of A30P seeds have a similar conformation to that of A30P fibrils. WT or A30P monomer showed very weak immunoreactivities to syn1–10 and syn75–91 (supplemental Fig. 2, *C*, *E*, and *I*). WT fibrils showed comparatively strong immunoreactivities to all three antibodies, whereas A30P fibrils showed a distinct pattern (supplemental Fig. 2, *D*, *F*, and *I*), being labeled strongly with syn1–10 but hardly at all with syn75–91.

Comparison of Protease-resistant Cores of WT and A30P α-Synuclein Fibrils—In order to investigate the structural differences between WT and A30P fibrils and also between WT fibrils formed in the presence of WT seeds and WT fibrils formed in the presence of A30P seeds, we analyzed protease-resistant cores of these fibrils after digestion with trypsin or proteinase K. Amyloid fibrils in neurodegenerative diseases and other types of amyloidosis are known to be highly resistant to many proteases, and the analysis of protease-resistant cores is frequently used for investigating the structures of various amyloid fibrils (34–36).

When monomeric α-synuclein was digested with trypsin or proteinase K, no band was detected (Fig. 5*A*). In contrast, 8–12 kDa core bands remained when the fibrils were treated with trypsin or proteinase K. Trypsin digestion of the fibrils composed of WT afforded two major bands of 10 and ~13 kDa (*black arrowheads*), and a similar band pattern was observed after the digestion of the WT fibrils formed in the presence of the WT seeds. On the other hand, two major bands of 9.5 and ~12.5 kDa (*white arrowheads*) with smaller molecular weights than those of the WT bands were detected after the digestion of A30P fibrils and WT fibrils formed in the presence of A30P seeds (Fig. 5, *B* and *C*). Similarly, digestion of WT fibrils and WT fibrils formed in the presence of WT seeds with proteinase K, a nonspecific protease, showed three major bands of 10–12 kDa (*black arrowheads*), whereas one major band of ~11.5 kDa (*white arrowhead*) was detected after the digestion of A30P fibrils and WT fibrils formed in the presence of A30P seeds (Fig. 5, *B* and *C*). These protein-chemical data strongly suggest that the core structures of A30P fibrils and WT fibrils formed in the presence of A30P seeds are distinct from those of WT fibrils and WT fibrils formed in the presence of WT seeds and further support the immunochemical results described above.

Effect of WT Seeds on Fibrillization of A30P Mutant α-Synuclein—Since WT α-synuclein assembles into fibrils faster than A30P mutant α-synuclein *in vitro* (Fig. 1*A*), WT seeds may be formed earlier than A30P seeds in the brains of

Effect of A30P Mutation on Fibrillization of α-Synuclein

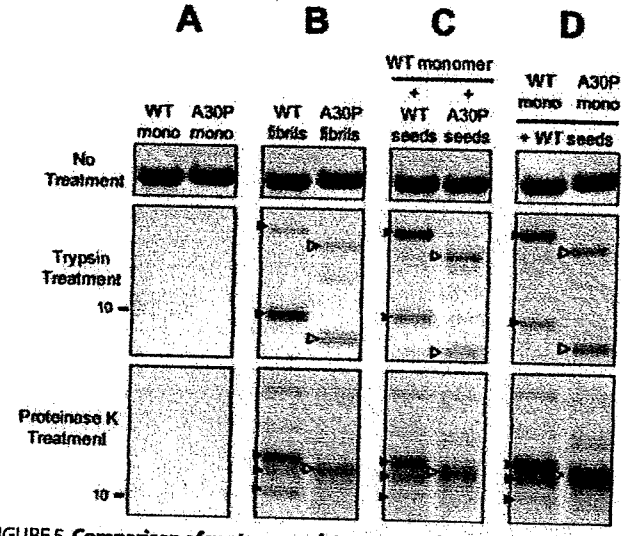

FIGURE 5. **Comparison of protease-resistant cores of WT fibrils, A30P fibrils, WT fibrils formed in the presence of A30P seeds, and A30P fibrils formed in the presence of WT seeds.** Monomeric WT and A30P α-synuclein (*A*), preformed WT and A30P fibrils (*B*), WT fibrils formed in the presence of WT seeds or A30P seeds (*C*), or WT or A30P fibrils formed in the presence of WT seeds (*D*) were treated with trypsin (final 50 μg/ml) or proteinase K (final 2 μg/ml) for 30 min and subjected to SDS-PAGE. Bands were stained with CBB. Note that protease-resistant band patterns of WT fibrils formed with WT seeds are the same as those of WT fibrils (*black arrowheads*), whereas the band patterns of WT fibrils formed with A30P seeds and A30P fibrils formed in the presence of WT seeds are the same as those of A30P seeds (*white arrowheads*). A typical experiment is shown; similar results were obtained in three separate experiments.

patients with the A30P mutation. We therefore investigated whether A30P mutant α-synuclein can assemble into fibrils in the presence of WT seeds and whether the A30P fibrils formed in the presence of WT seeds show the characteristics of WT fibrils. Nucleation-dependent fibrillization of A30P mutant α-synuclein was observed in the presence of WT seeds. When the A30P fibrils formed in the presence of WT seeds were analyzed by electron microscopy and ultracentrifugation (Fig. 6), the A30P fibrils formed in the presence of WT seeds appeared to be morphologically indistinguishable from the WT fibrils formed in the presence of WT seeds before the preparation of suspensions (Fig. 6*A*, *i* and *ii*). However, after suspension, many tiny fibrils were observed in the A30P fibrils formed in the presence of WT seeds, whereas such short fibrils were hardly detected in the WT fibrils formed in the presence of WT seeds (Fig. 6*A*, *iii* and *iv*). This was confirmed by measuring the length of fibrils in these suspensions prepared by pipetting (supplemental Fig. 3. Many tiny fibrils were observed in the supernatant of A30P fibrils formed in the presence of WT seeds, whereas such tiny fibrils were hardly detected in the supernatant of WT fibrils formed in the presence of WT seeds (Fig. 6*A*, *v* and *vi*). Quantitative analysis of α-synuclein in the supernatants and pellets by SDS-PAGE confirmed the results of EM observation; more α-synuclein was detected in the supernatant of A30P fibrils formed in the presence of WT seeds than in that of WT fibrils formed in the presence of WT seeds (Fig. 6, *B* and *C*). These results indicate that A30P fibrils formed in the presence of WT seeds do not acquire the character of the WT seeds but retain the character of A30P fibrils.

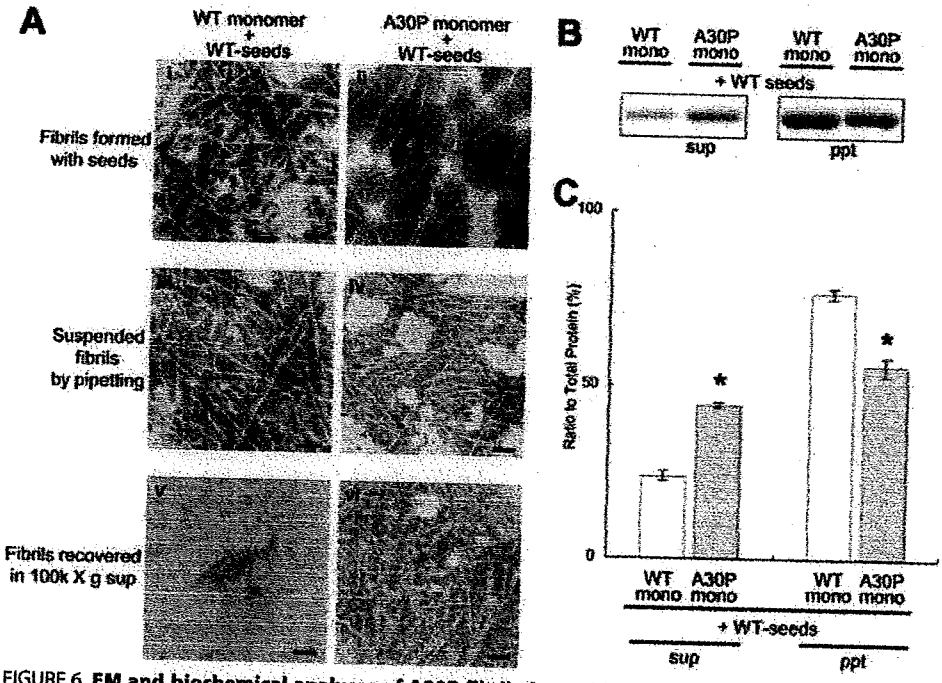

FIGURE 6. **EM and biochemical analyses of A30P fibrils formed in the presence of WT seeds.** *A*, EM analysis of WT fibrils formed in the presence of WT seeds (*i*, *iii*, and *v*) and A30P fibrils formed in the presence of WT seeds (*ii*, *iv*, and *vi*) before and after suspension. Negatively stained WT or A30P fibrils formed in the presence of WT seeds (*i* and *ii*), the fibrils after suspension (*iii* and *iv*), and the fibrils in the supernatants after centrifugation (*v* and *vi*) were observed by electron microscopy. *Scale bar*, 200 nm. *B*, CBB staining of α-synuclein recovered in the supernatants and the pellets after centrifugation of the fibrils. *C*, quantification of α-synuclein recovered in the supernatants and pellets after ultracentrifugation (expressed as a percentage of total α-synuclein, taken as 100%). The results are expressed as means ± S.E. ($n = 3$) (*, $p < 0.01$).

Conformation of A30P Fibrils Formed in the Presence of WT Seeds—To investigate the relationship between the shedding propensity of fibrils and conformation, we analyzed A30P fibrils formed in the presence of WT seeds by dot blot assay using the epitope-specific antibodies (Fig. 7). Surprisingly, A30P fibrils formed in the presence of WT seeds showed the same pattern of immunoreactivity as A30P fibrils, and the pattern was different from that of WT fibrils formed in the presence of WT seeds (Fig. 7, *C*, *D*, *E*, *F*, and *I*). Similar results were obtained with number 36 and NAC2 antibodies (data not shown).

To further investigate the structural differences between WT fibrils formed in the presence of WT seeds and A30P fibrils formed in the presence of WT seeds, the protease-resistant cores of the fibrils were analyzed. As shown in Fig. 5, *B* and *D*, the band patterns of the trypsin- and proteinase K-resistant cores of A30P fibrils formed in the presence

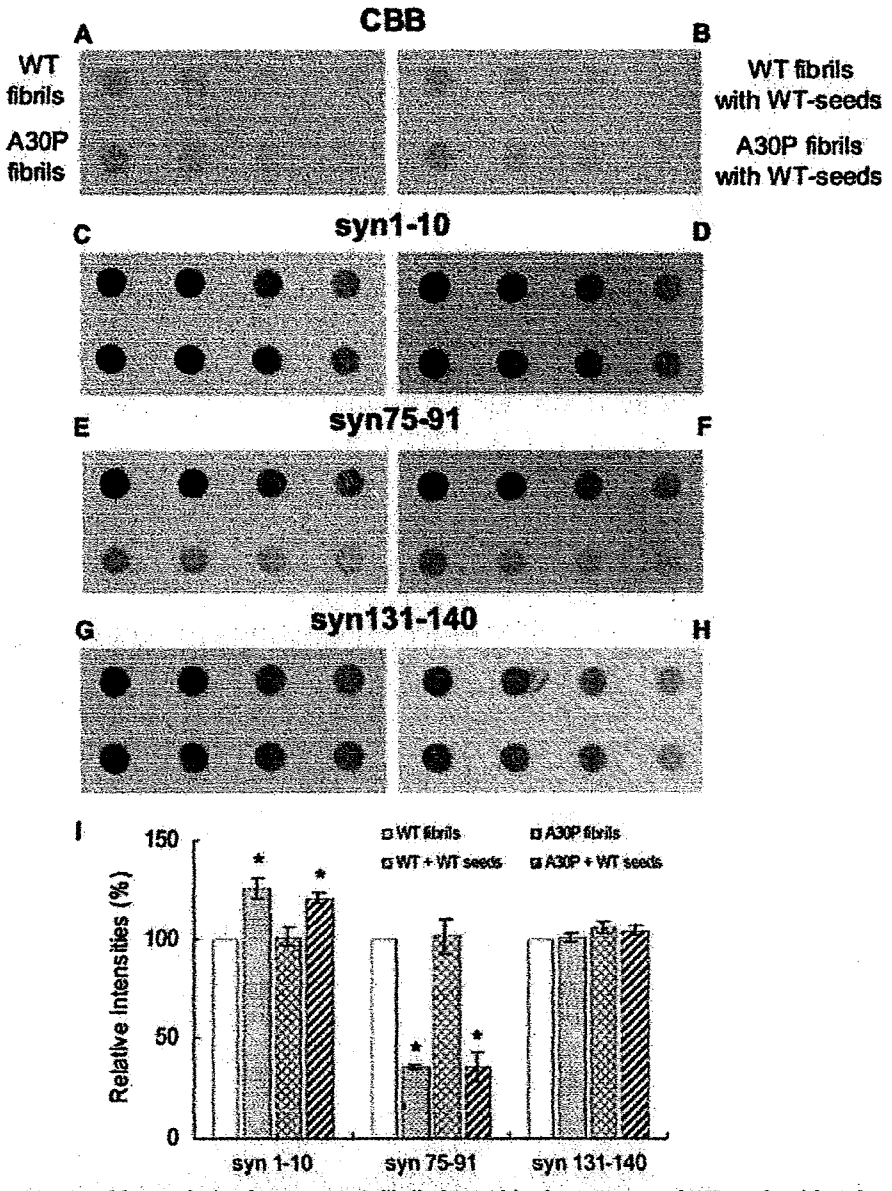

FIGURE 7. **Dot blot analysis of WT or A30P fibrils formed in the presence of WT seeds with epitope-specific antibodies.** Equal amounts of WT and A30P fibrils, WT fibrils formed in the presence of WT seeds, and A30P fibrils formed in the presence of WT seeds were spotted on polyvinylidene difluoride membrane and stained with CBB (*A* and *B*) or immunodetected with syn1–10 (*C* and *D*), syn75–91 (*E* and *F*), or syn131–140 antibodies (*G* and *H*). For CBB staining and dot blotting with syn74–91, 100, 50, 25, and 12.5 ng of protein were spotted. For immunodetection with syn1–10 and syn131–140, 10, 5, 2.5, and 1.25 ng of protein were spotted. A typical experiment is shown; similar results were obtained in three separate experiments. *I*, quantification of immunoreactivities of WT fibrils, A30P fibrils, and WT or A30P fibrils formed in the presence of WT seeds. The results are expressed as a percentage of immunoreactivity of WT fibrils, taken as 100% (means ± S.E., $n = 3$) (*, $p < 0.01$).

of WT seeds were the same as those of A30P fibrils (*white arrowheads*) and distinct from those of WT fibrils and WT fibrils formed with WT seeds (*black arrowheads*). These results strongly support the view that A30P fibrils formed in the presence of WT seeds do not acquire the conformation of the WT seeds but retain the conformation of A30P fibrils.

Cytotoxicities of WT and Mutant α-Synuclein Fibrils—To investigate the relationship between the shedding propensity of fibrils and the cytotoxicity, SH-SY5Y cells were treated with WT or mutant fibrils (suspended by pipetting or sonication), and the cytotoxicity was determined by an MTT reduction assay, as has been used widely. As shown in Fig. 8*A*, all fibrils composed of WT or mutant α-synuclein showed a significant reduction of MTT ($p < 0.01$), whereas no toxicity was detected with monomeric WT or mutant α-synuclein. Interestingly, A30P fibrils showed a stronger effect than WT fibrils or the other mutant fibrils, suggesting a link between shedding propensity and cytotoxicity. When cells were treated with sonicated fibrils, which were fragmented homogeneously to short fibrils (data not shown), the cytotoxicity was significantly enhanced ($p < 0.01$), although the increase was small in the case of the E46K mutant (Fig. 8*A*). These results indicate that large numbers of short fibrils are more toxic than small numbers of long fibrils. It is possible that short fibrils can interact with cell membranes more easily than long fibrils. The cytotoxicities of WT fibrils formed in the presence of A30P seeds and A30P fibrils formed in the presence of WT seeds were also analyzed by MTT assay (Fig. 8*B*). These fibrils with increased shedding propensity showed stronger cytotoxicity than WT fibrils formed in the presence of WT seeds, and sonication enhanced the toxic effects of these fibrils. These data demonstrate a close correlation between the shedding propensity of fibrils and the cytotoxicity.

DISCUSSION

Nucleation-dependent aggregation has been reported to play a role in the fibrillization of many amyloidogenic proteins, including Aβ protein, β2-microglobulin, and apoA-II (37–39). Assembly of α-synuclein into fibrils has also been shown to be a nucleation-dependent process (22). In this study, we have extensively investigated the nucleation-dependent assembly of WT and mutant α-synuclein into fibrils, the shedding properties of these fibrils, and the conformational differences between WT and A30P fibrils and between these fibrils formed in the presence of different seeds. The addition of A30P seeds to WT monomer promoted the fibrillization of WT α-synuclein, indicating that A30P fibrils have a cross-seeding effect on WT α-synuclein. Surprisingly, A30P seeds promoted the fibrillization of WT

Effect of A30P Mutation on Fibrillization of α-Synuclein

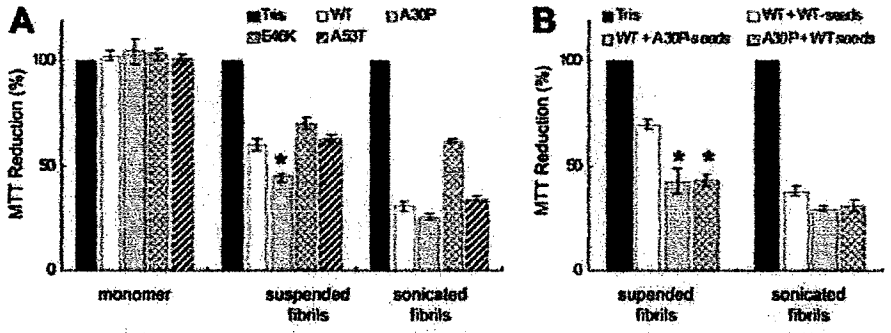

FIGURE 8. **Cytotoxicities of WT and mutant α-synuclein fibrils.** *A*, SH-SY5Y cells were treated with monomeric WT or mutant α-synuclein, suspended fibrils, or sonicated fibrils, and cellular damage was detected by an MTT reduction assay. Significant reduction of MTT was detected in cells treated with WT and mutant fibrils ($p > 0.01$), whereas no toxicity was detected in the case of monomeric α-synuclein. *B*, cytotoxic effects of WT fibrils formed in the presence of WT seeds or A30P seeds and A30P fibrils formed in the presence of WT seeds (suspended or sonicated). The results are presented as percentage MTT reduction, with the values obtained upon the addition of 30 mM Tris-HCl, pH 7.5, taken as 100%. The results are expressed as means ± S.E. ($n = 3$) (*, $p < 0.01$).

faster than did WT, E46K, and A53T seeds. In contrast, the seeding effect of A53T seeds on WT α-synuclein was similar to that of WT seeds, and that of E46K seeds was much smaller. EM and ultracentrifugation studies revealed that the strong seeding effect of A30P was due to the enhanced shedding propensity of A30P fibrils. A similar effect of amyloid fibrils has been found in studies of yeast prion protein (Sup35) (40). Sup35 N-terminal residues 1–254 (SupNM) assembled into amyloid fibrils with different conformations, Sc4 or Sc37, upon incubation at 4 or 37 °C, respectively. Sc4 had a higher fragility than Sc37, and only Sc4 amyloid had high infectivity and seeding efficacy for fibrillization of Sup35 monomer. Furthermore, it has been reported that pathological prion protein can be detected sensitively by cyclic amplification of protein misfolding with sonication (41). These reports demonstrate that fragmentation or shedding of amyloid fibrils can accelerate fibrillization and result in high infectivity and are therefore consistent with our findings here. Substitution of alanine to proline at residue 30 may have a significant effect on the conformation of α-synuclein monomer and assembled fibrils. Proline introduces a bend in the peptide chain, abolishing α-helix structure and disrupting β-sheets. It has been shown that in the A30P mutant, a region of helical structure (residues 18–31) that exists in WT is abolished, formation of β-sheet-rich mature fibril structure is retarded, and the polypeptide backbone stiffness (segment length of about 5 residues) is increased (42, 43). Since the A30P mutation exists in the vicinity of the N terminus of the fibril core (residues 31–109) (34), it is reasonable to speculate that the proline residue would affect both fibrillization and the conformation of the fibrils.

To investigate whether the structural and biochemical features of A30P fibrils can be transmitted to WT fibrils formed in the presence of A30P seeds, we analyzed the fibrils by electron microscopy, ultracentrifugation, dot blot assay, and protease-resistant core analysis. The results clearly demonstrated that the unique features of A30P fibrils were transmitted to WT fibrils grown in the presence of A30P seeds. Transmission of structures and features of fibrils has been reported in other amyloidogenic proteins, such as prion proteins and Aβ. When amyloid fibrils of Syrian hamster prion protein were added to mouse prion protein, the mouse prion protein formed Syrian hamster-type amyloid fibrils but not mouse-type fibrils (44). A similar effect has been seen with yeast prion protein and Aβ (45, 46).

In this study, we have employed a novel method using epitope-specific antibodies of α-synuclein to detect structural difference between WT fibrils and A30P fibrils (Fig. 4). Dot blot analysis also revealed the presence of conformational differences between α-synuclein monomer and the fibrils (supplemental Fig. 2). WT fibrils were recognized very strongly by antibodies to the N-terminal region and NAC region, whereas the monomers were only weakly recognized by these antibodies. Since the N-terminal region and C-terminal region of α-synuclein show intramolecular long range interactions (15), it is reasonable that antibodies to the N terminus and NAC region cannot access the epitopes in the monomer. The results also suggest that the N-terminal and NAC regions of α-synuclein are both exposed at the surface in the fibrils (supplemental Fig. 2, *D*, *F*, and *I*). In A30P, however, the NAC region is buried in the fibrils (supplemental Fig. 2, *F* and *I*), probably because the bent N terminus masks the NAC region and blocks recognition by the corresponding antibody. Recent single molecule studies *in vitro* have shown that under conditions similar to physiological, α-synuclein exists as three distinct conformers that are characterized by long distance weak interactions, random coil structure, and β-like structure and that the relative abundance of β-like conformer is increased in A30P mutant (47). This is in good agreement with our observations by dot blot assay of WT and A30P monomeric α-synuclein with epitope-specific antibodies.

In this study, fibrillization of the A30P monomer was slower than that of WT, but the seeding effect of A30P on the fibrillization was stronger than that of WT. This reciprocal effect of A30P monomer and the fibrils may explain the different results in the aggregation experiments.

In the EM and biochemical analyses of seeds, we found that small fibril fragments are recovered in the supernatant of A30P fibrils and that these fragments act as seeds. This is surprising, because the supernatant after ultracentrifugation is normally referred to as the soluble fraction in biochemistry. Some reports have suggested the presence of nonfibrillar soluble oligomers or abnormal species in the soluble fractions of diseased brains. It is possible that such soluble oligomers or abnormal species may correspond to small fibrils or fragments.

In this *in vitro* study, we found an important effect of A30P mutation, which may provide a clue for understanding the mechanism of early onset in patients harboring the A30P mutation. Our schematic models of nucleation-dependent fibrillization are shown in Fig. 9. WT fibrils formed in the presence of A30P seeds possess the structural and functional characteristics of A30P fibrils (Fig. 9*A*), whereas A30P fibrils formed in the presence of WT seeds do not acquire the character of the WT seeds but retain the features of A30P fibrils (Fig. 9*B*). Recent

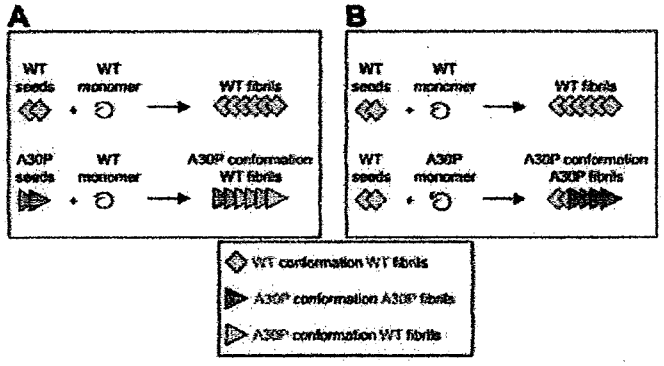

FIGURE 9. **Schematic illustration of proposed nucleation-dependent fibrillization of WT and A30P mutant α-synuclein.** *A*, fibrillization of WT α-synuclein in the presence of WT seeds or A30P seeds. When WT seeds are added to WT monomer, WT fibrils are formed (*top*). When A30P seeds are added to WT monomer, WT fibrils with the character and conformation of A30P fibrils are formed (*bottom*). *B*, fibrillization of A30P α-synuclein in the presence of WT seeds. When WT seeds are added to A30P monomer, A30P fibrils with the usual A30P fibril conformation are formed.

immunohistochemical analyses of the brains of PD patients who underwent transplantation have shown that α-synuclein lesions can propagate from host to grafted cells (48, 49). Thus, fibrillization of α-synuclein in the brains of patients with A30P mutation may also be faster than in normal brains. We would like to investigate this possibility in the future.

REFERENCES

1. Spillantini, M. G., Crowther, R. A., Jakes, R., Hasegawa, M., and Goedert, M. (1998) *Proc. Natl. Acad. Sci. U. S. A.* **95,** 6469–6473
2. Baba, M., Nakajo, S., Tu, P. H., Tomita, T., Nakaya, K., Lee, V. M., Trojanowski, J. Q., and Iwatsubo, T. (1998) *Am. J. Pathol.* **152,** 879–884
3. Fujiwara, H., Hasegawa, M., Dohmae, N., Kawashima, A., Masliah, E., Goldberg, M. S., Shen, J., Takio, K., and Iwatsubo, T. (2002) *Nat. Cell Biol.* **4,** 160–164
4. Polymeropoulos, M. H., Lavedan, C., Leroy, E., Ide, S. E., Dehejia, A., Dutra, A., Pike, B., Root, H., Rubenstein, J., Boyer, R., Stenroos, E. S., Chandrasekharappa, S., Athanassiadou, A., Papapetropoulos, T., Johnson, W. G., Lazzarini, A. M., Duvoisin, R. C., Di Iorio, G., Golbe, L. I., and Nussbaum, R. L. (1997) *Science* **276,** 2045–2047
5. Kruger, R., Kuhn, W., Muller, T., Woitalla, D., Graeber, M., Kosel, S., Przuntek, H., Epplen, J. T., Schols, L., and Riess, O. (1998) *Nat. Genet.* **18,** 106–108
6. Zarranz, J. J., Alegre, J., Gomez-Esteban, J. C., Lezcano, E., Ros, R., Ampuero, I., Vidal, L., Hoenicka, J., Rodriguez, O., Atares, B., Llorens, V., Gomez Tortosa, E., del Ser, T., Munoz, D. G., and de Yebenes, J. G. (2004) *Ann. Neurol.* **55,** 164–173
7. Singleton, A. B., Farrer, M., Johnson, J., Singleton, A., Hague, S., Kachergus, J., Hulihan, M., Peuralinna, T., Dutra, A., Nussbaum, R., Lincoln, S., Crawley, A., Hanson, M., Maraganore, D., Adler, C., Cookson, M. R., Muenter, M., Baptista, M., Miller, D., Blancato, J., Hardy, J., and Gwinn-Hardy, K. (2003) *Science* **302,** 841
8. Farrer, M., Kachergus, J., Forno, L., Lincoln, S., Wang, D. S., Hulihan, M., Maraganore, D., Gwinn-Hardy, K., Wszolek, Z., Dickson, D., and Langston, J. W. (2004) *Ann. Neurol.* **55,** 174–179
9. Chartier-Harlin, M. C., Kachergus, J., Roumier, C., Mouroux, V., Douay, X., Lincoln, S., Levecque, C., Larvor, L., Andrieux, J., Hulihan, M., Waucquier, N., Defebvre, L., Amouyel, P., Farrer, M., and Destee, A. (2004) *Lancet* **364,** 1167–1169
10. Ibanez, P., Bonnet, A. M., Debarges, B., Lohmann, E., Tison, F., Pollak, P., Agid, Y., Durr, A., and Brice, A. (2004) *Lancet* **364,** 1169–1171
11. Nishioka, K., Hayashi, S., Farrer, M. J., Singleton, A. B., Yoshino, H., Imai, H., Kitami, T., Sato, K., Kuroda, R., Tomiyama, H., Mizoguchi, K., Murata, M., Toda, T., Imoto, I., Inazawa, J., Mizuno, Y., and Hattori, N. (2006) *Ann. Neurol.* **59,** 298–309
12. Fuchs, J., Nilsson, C., Kachergus, J., Munz, M., Larsson, E. M., Schule, B., Langston, J. W., Middleton, F. A., Ross, O. A., Hulihan, M., Gasser, T., and Farrer, M. J. (2007) *Neurology* **68,** 916–922
13. Davidson, W. S., Jonas, A., Clayton, D. F., and George, J. M. (1998) *J. Biol. Chem.* **273,** 9443–9449
14. Uversky, V. N., Li, J., and Fink, A. L. (2001) *J. Biol. Chem.* **276,** 10737–10744
15. Bertoncini, C. W., Jung, Y. S., Fernandez, C. O., Hoyer, W., Griesinger, C., Jovin, T. M., and Zweckstetter, M. (2005) *Proc. Natl. Acad. Sci. U. S. A.* **102,** 1430–1435
16. Spillantini, M. G., Schmidt, M. L., Lee, V. M., Trojanowski, J. Q., Jakes, R., and Goedert, M. (1997) *Nature* **388,** 839–840
17. Serpell, L. C., Berriman, J., Jakes, R., Goedert, M., and Crowther, R. A. (2000) *Proc. Natl. Acad. Sci. U. S. A.* **97,** 4897–4902
18. Crowther, R. A., Daniel, S. E., and Goedert, M. (2000) *Neurosci. Lett.* **292,** 128–130
19. Biere, A. L., Wood, S. J., Wypych, J., Steavenson, S., Jiang, Y., Anafi, D., Jacobsen, F. W., Jarosinski, M. A., Wu, G. M., Louis, J. C., Martin, F., Narhi, L. O., and Citron, M. (2000) *J. Biol. Chem.* **275,** 34574–34579
20. Giasson, B. I., Murray, I. V., Trojanowski, J. Q., and Lee, V. M. (2001) *J. Biol. Chem.* **276,** 2380–2386
21. Conway, K. A., Harper, J. D., and Lansbury, P. T. (1998) *Nat. Med.* **4,** 1318–1320
22. Narhi, L., Wood, S. J., Steavenson, S., Jiang, Y., Wu, G. M., Anafi, D., Kaufman, S. A., Martin, F., Sitney, K., Denis, P., Louis, J. C., Wypych, J., Biere, A. L., and Citron, M. (1999) *J. Biol. Chem.* **274,** 9843–9846
23. Conway, K. A., Lee, S. J., Rochet, J. C., Ding, T. T., Williamson, R. E., and Lansbury, P. T., Jr. (2000) *Proc. Natl. Acad. Sci. U. S. A.* **97,** 571–576
24. Conway, K. A., Harper, J. D., and Lansbury, P. T., Jr. (2000) *Biochemistry* **39,** 2552–2563
25. Greenbaum, E. A., Graves, C. L., Mishizen-Eberz, A. J., Lupoli, M. A., Lynch, D. R., Englander, S. W., Axelsen, P. H., and Giasson, B. I. (2005) *J. Biol. Chem.* **280,** 7800–7807
26. Goldberg, M. S., and Lansbury, P. T., Jr. (2000) *Nat. Cell Biol.* **2,** E115–E119
27. Volles, M. J., and Lansbury, P. T., Jr. (2002) *Biochemistry* **41,** 4595–4602
28. Jensen, P. H., Nielsen, M. S., Jakes, R., Dotti, C. G., and Goedert, M. (1998) *J. Biol. Chem.* **273,** 26292–26294
29. Jo, E., Fuller, N., Rand, R. P., St George-Hyslop, P., and Fraser, P. E. (2002) *J. Mol. Biol.* **315,** 799–807
30. Wood, S. J., Wypych, J., Steavenson, S., Louis, J. C., Citron, M., and Biere, A. L. (1999) *J. Biol. Chem.* **274,** 19509–19512
31. Masuda, M., Dohmae, N., Nonaka, T., Oikawa, T., Hisanaga, S., Goedert, M., and Hasegawa, M. (2006) *FEBS Lett.* **580,** 1775–1779
32. Taniguchi, S., Suzuki, N., Masuda, M., Hisanaga, S., Iwatsubo, T., Goedert, M., and Hasegawa, M. (2005) *J. Biol. Chem.* **280,** 7614–7623
33. Masuda, M., Suzuki, N., Taniguchi, S., Oikawa, T., Nonaka, T., Iwatsubo, T., Hisanaga, S., Goedert, M., and Hasegawa, M. (2006) *Biochemistry* **45,** 6085–6094
34. Miake, H., Mizusawa, H., Iwatsubo, T., and Hasegawa, M. (2002) *J. Biol. Chem.* **277,** 19213–19219
35. Aoyagi, H., Hasegawa, M., and Tamaoka, A. (2007) *J. Biol. Chem.* **282,** 20309–20318
36. Raymond, G. J., Hope, J., Kocisko, D. A., Priola, S. A., Raymond, L. D., Bossers, A., Ironside, J., Will, R. G., Chen, S. G., Petersen, R. B., Gambetti, P., Rubenstein, R., Smits, M. A., Lansbury, P. T., Jr., and Caughey, B. (1997) *Nature* **388,** 285–288
37. Naiki, H., Higuchi, K., Nakakuki, K., and Takeda, T. (1991) *Lab. Invest.* **65,** 104–110
38. Jarrett, J. T., and Lansbury, P. T., Jr. (1993) *Cell* **73,** 1055–1058
39. Naiki, H., and Gejyo, F. (1999) *Methods Enzymol.* **309,** 305–318
40. Tanaka, M., Collins, S. R., Toyama, B. H., and Weissman, J. S. (2006) *Nature* **442,** 585–589
41. Saborio, G. P., Permanne, B., and Soto, C. (2001) *Nature* **411,** 810–813
42. Lee, J. C., Langen, R., Hummel, P. A., Gray, H. B., and Winkler, J. R. (2004)

Proc. Natl. Acad. Sci. U. S. A. **101,** 16466–16471
43. Bussell, R., Jr., and Eliezer, D. (2001) *J. Biol. Chem.* **276,** 45996–46003
44. Jones, E. M., and Surewicz, W. K. (2005) *Cell* **121,** 63–72
45. Petkova, A. T., Leapman, R. D., Guo, Z., Yau, W. M., Mattson, M. P., and Tycko, R. (2005) *Science* **307,** 262–265
46. Tanaka, M., Chien, P., Yonekura, K., and Weissman, J. S. (2005) *Cell* **121,** 49–62
47. Sandal, M., Valle, F., Tessari, I., Mammi, S., Bergantino, E., Musiani, F., Brucale, M., Bubacco, L., and Samorì, B. (2008) *PLoS Biol.* **6,** e6
48. Li, J. Y., Englund, E., Holton, J. L., Soulet, D., Hagell, P., Lees, A. J., Lashley, T., Quinn, N. P., Rehncrona, S., Bjorklund, A., Widner, H., Revesz, T., Lindvall, O., and Brundin, P. (2008) *Nat. Med.* **14,** 501–503
49. Kordower, J. H., Chu, Y., Hauser, R. A., Freeman, T. B., and Olanow, C. W. (2008) *Nat. Med.* **14,** 504–506